Aus dem Max-Delbrück-Center for Molecular Medicine, Cellular Neuroscience

DISSERTATION

Astrocytes control GABAergic inhibition of neurons in the mouse barrel cortex

zur Erlangung des akademischen Grades

Philosophiae Doctor (PhD) in Medical Neurosciences

International Graduate Program Medical Neurosciences, Charité Universitätsmedizin Berlin.

Von Bruno Benedetti,

Aus Trieste, Italia

Gutachter: 1. Prof. Dr. H. Kettenmann
2. Prof. Dr. rer. nat. D. Feldmeyer
3. Prof. Dr. A. Verkhratsky

Datum der Promotion: 24.02.2012

ABSTRACT

Astrocytes in the barrel cortex respond with an increase in transient calcium (Ca^{2+}) to neuronal stimulation. This response is restricted to the stimulated barrel field. In the present study we suppressed the astrocyte response by dialyzing these cells with the Ca^{2+} chelator BAPTA. Electrical stimulation triggered a depolarization in stellate or pyramidal “regular spiking”, neurons from cortex layer 4 and 2/3. This response was also augmented in amplitude and duration after astrocytes were dialyzed with BAPTA. Combined blockade of $GABA_A$ and $GABA_B$ receptors mimicked the effect of BAPTA dialysis, while glutamate receptor blockers had no effect. Moreover, the frequency of spontaneous postsynaptic currents was increased after BAPTA dialysis. Outside the range of BAPTA dialysis, the astrocytes responded with a Ca^{2+} increase, but, in contrast to control, the response was no longer restricted to one barrel field. Our findings indicate that astrocytes control neuronal inhibition in the barrel cortex.

Keywords: astrocyte, barrel cortex, calcium, neuron-glia interaction, inhibition

Abbreviations:

STM depol: Stimulus-evoked depolarization

Half rep: time for half repolarization

ISTM: integral of stimulus-evoked depolarization

Other abbreviations:

ACSF: artificial cerebro-spinal fluid **BAPTA:** 1,2-bis (o-aminophenoxy) ethane-N,N,N',N'-tetraacetic acid **Ca^{2+}:** calcium **Cy3**: Cyanine dye 3 **CPT:** 8-Cyclopentyl-1,3-dimethylxanthine (CPT) **D-AAO**: D-amino acid oxidase **E_m**: membrane potential **eGFP**: enhanced Green Fluorescent Protein **GABA:** γ-aminobutirric acid **GFAP**: Glial Fibrillary Acidic Protein **GAT:** GABA transporter **IP3:** inositol 1-3 triphosphate **L2/3,**: cortex layer 2/3 **L4**: cortex layer 4) **mGluR:** metabotropic glutamate receptor **MPEP:** 2-Methyl-6-(phenylethynyl) pyridine hydrochloride **mRFP**: murine Red Fluorescent Protein **PBS**: Phosphate Buffer Solution **STM:** stimulus **TX-100**: Triton X 100

INTRODUCTION

Barrel Cortex Anatomy

This dissertation focuses on the functional interactions between neurons and astrocytes in the barrel cortex. The barrel cortex is a well-defined area of the parietal cortex and forms part of the somatosensory cortex in most rodents' brains. The neurons in the barrel cortex receive tactile information as perceived through the whiskers, which deflect both passively in response to external stimulation and actively due to exploratory movements known as 'whisking'. The barrel cortex represents about 13% of the total cortex area and 69% of the somatosensory cortex (Lee & Erzurumlu, 2005) extending for approximately 2 to 3 mm^2 (Woolsey & Van der Loos, 1970), (Welker & Woolsey, 1974). The neuronal pathway connecting the snout's whiskers to the barrel cortex travels through the brain-stem, thalamus, and then terminates primarily in the fourth cortex-layer, to be then further processed into other cortical layers (Agmon & Connors, 1991), (Agmon & Connors, 1992), (Lubke & Feldmeyer, 2007). Most of the brain cortex is composed of six horizontal layers, numbered progressively from the outside-in. The somatosensory cortex is also organized in vertical columns which represent its sensory units. In the barrel cortex each column responds to the movement of a single whisker (Lubke & Feldmeyer, 2007). Each column's coordinates match the relative whisker's respective position on the snout in a so called "somatotopic" fashion. The somatotopic structure of the barrel cortex can be highlighted by cytochrome oxidase staining in which each column appears as a black square (barrel). Cytochrome oxidase preferentially marks the mitochondria in the

neuronal synapses, which are more abundant at the center of each column (Simons & Woolsey, 1984), (Land & Simons, 1985). The “barrel cortex” owes its name to this peculiar honeycomb-like pattern. The barrels are also visible in a fresh brain preparation without staining but with a slightly different appearance. In coronal brain slices, the barrels appear in layer 4 as bright squares (interseptae) separated by darker areas (septae) (Feldmeyer et al., 1999). This phenomenon is emphasized by misalignment of the microscope’s light-beam (Agmon & Connors, 1991), (Agmon & Connors, 1992) so that its pathway is not orthogonal to the slice sample. In fresh preparations, the barrel pattern is caused by a higher density of neurites in the interseptae, and of cell somata in the septae. It has been speculated that such distribution of somata and processes would create an irregular light-diffraction accounting for the particular appearance of barrel layer 4. Barrels are a feature of whiskered animals but are not present in all mammalians. However, their morphological and functional organization broadly resembles other mammalian sensory cortices (Mountcastle, 1997). In all other cortex regions, the column pattern is undistinguishable, at least in fresh tissue preparations. The possibility to see the exact location of each cortical column was therefore helpful for our functional studies that required the use of fresh tissue. The advantage of using the barrel cortex as a model for our experiments was also in the predictability of functional activation of single columns upon local stimulation. Furthermore, glial cell activity in response to local stimulation has been thoroughly characterized in this context (Wang et al. 2006, Schipke et al. 2008).

Cellular components of the barrel cortex

Neuronal cells

Glutamate is the major excitatory neurotransmitter in the cortex. Glutamatergic neurons have been well characterized in their morphology and connectivity (Feldmeyer et al., 1999), (Lubke et al., 2000), (Lubke et al., 2003), (Feldmeyer, Roth & Sakmann, 2005), (Lubke & Feldmeyer, 2007). They are conventionally grouped into three morphological categories: spiny stellate neurons, star-pyramidal, and pyramidal neurons.

Spiny stellate neurons owe their name to the star-like distribution (stellate) of their dendrites as well as to the high density of their synaptic spines (spiny). Their somata are located in the barrel layer 4, mostly in the septae; their dendrites are preferentially directed toward a single adjacent interseptum. As a result of this arrangement, their overall morphology appears typically anisotropic (Feldmeyer et al., 1999). Spiny stellate neurons largely project their axons toward the *pia mater* to contact layer 2/3 neurons within the same barrel column (Lubke et al. 2003). Each individual spiny stellate cell provides only a weak contribution to layer 2/3 excitation so that the simultaneous activity of several neurons in layer 4 is necessary for efficient signal transmission (Feldmeyer et al., 2002). Spiny stellate axonal projections also span throughout all the other cortical layers and collateral projections in layer 5 and in layer 6, they reach over neighboring columns (Lubke et al., 2000). Local projections within a barrel contact other neurons in layer 4 within a given column. In this region, they provide a reliable network for the propagation and amplification of the input they receive from the thalamic afferents (Feldmeyer et al., 1999).

Star-pyramidal neurons are another type of excitatory neurons in layer 4. They are morphologically similar to spiny stellate cells, but they are endowed with a main vertical dendrite extending toward layer 2/3 while lacking anisotropy (Feldmeyer et al., 1999). Their axons extend vertically across all cortex layers, mostly oriented in wider columns than those of spiny stellate neurons. Axonal branches occasionally extend to neighboring barrels. Axons also tend to form clusters in layer 2/3 (Lubke et al., 2000).

Pyramidal neurons are excitatory cells of the cortex layer 2/3 and 5. Their apical dendrites extend vertically to the *pia mater*. They end in tufts and their branching is most prominent close to the cortical surface. Their synapses are mainly intracolumnar: excitatory innervations of layer 2/3 rise from layer 4; synaptic contacts are also formed locally with other layer 2/3 neurons of the same barrel. The local connections within layer 2/3 amplify the excitation rising from layer 4; this could act as an excitatory feedback mechanism within a given barrel (Feldmeyer, Lubke & Sakmann, 2006). Axonal projections of pyramidal neurons extend vertically through all cortical layers. Collateral projections reach across neighboring barrels, mainly in layer 2/3 and layer 5 (Lubke et al. 2003).

γ-aminobutirric acid (GABA) is the major inhibitory neurotransmitter in the cortex. GABA is released from the interneurons which are morphologically very heterogeneous. Some authors recently grouped the cortical interneurons on the base of cluster analysis (Helmstaedter, Sakmann & Feldmeyer, 2009), (Helmstaedter et al., 2009). Considering their axonal projections, layer 2/3 interneurons could be grouped into intralaminar, lateral and local-projecting (Helmstaedter et al., 2009). Another clustering was based on their dendritic

polarity whereby the number of primary dendrites was shown to correlate with the intrinsic electric excitability. This could be used as a further criterion for classification. The dendritic polarity index of layer 2/3 cells determined the existence of seven interneuronal categories. Such classification was applied only recently to layer 2/3 cells and has clear advantages from the perspective of functional studies. Starting in the early twentieth century, interneurons have been studied and classified by the following conventional categories: basket cells, chandelier cells, double bouquet, bitufted, Martinotti cells, Cajal-Retius cells and neurogliaform cells (Fox, 2008), (Markram et al*,* 2009).

Basket cells, described in early works by Ramon y Cajal in 1911, are mostly located in layers 3 and 5. According to the shape of their somata, dendritic extensions, and innervation domains, basket cells are divided into three categories: small basket, large basket and nest basket cells (Wang et al., 2002). Their synaptic targets are the somata and dendrites of pyramidal cells. Small basket cells have sparse branching limited to a single column domain while large basket cells reach neighboring columns. Nest basket cells have an irregular arborization and “nest-like appearance.” They also have hybrid features in their axonal projections resembling both small and large basket cells.

Chandelier cells are the only interneurons targeting to axons. These cells respond to the overall barrel excitation suppressing the generation of action potentials (AP) and limiting the glutamate release from excitatory neurons. This reduces the overall barrel excitability as well as the amount of positive feedback (Zhu, Stornetta & Zhu, 2004). Chandelier cells are found in layers 2 and 6. Their number increases and their morphology grows more complex in “higher” species such as primates (DeFelipe, 1999), (DeFelipe, 2002).

Double bouquet (layer 2/3) and bipolar cells (layers 2 to 5) are dendrite-targeting interneurons with bundle-like longitudinal projections resembling a “horse tail” and thicker lateral projections that can extend across all layers (Peters & Harriman, 1988) (Keller & White, 1987), (Somogyi & Cowey, 1981), (DeFelipe et al., 1990).

Similarly to bipolar cells, bitufted cells (layers 2/3 and 4) are endowed with bipolar longitudinal projections and have a wider, though less extensive, axonal branching. They mainly contact the dendrites of excitatory neurons (Somogyi et al., 1998).

Martinotti cells project vertically toward layer 1 and send collaterals across neighboring columns. They target predominantly apical dendrites of pyramidal neurons (Wang et al., 2004).

Cajal-Retzius cells are located in layer 1 and project laterally. Their processes span through several columns and target apical dendrites of pyramidal neurons (Radnikow, Feldmeyer & Lubke, 2002).

Neurogliaform neurons are highly symmetrical in their projections. Their processes branch close to the point of their emergence from the cell soma and are directed toward dendrites of neighboring neurons (Zhu et al., 2004).

Electric signature of excitatory and inhibitory neurons

Neurons can be characterized on the base of their AP firing. This is a quick and convenient method for cellular identification in patch clamp experiments although not as precise, for instance, as post-fixation immunostaining. Injection of electric current through a patch pipette leads the neuron to a tonic depolarization during which APs are fired. Excitatory neurons typically fire a slow-adapting train of spikes, a pattern known as “regular spiking” (Chagnac-Amitai & Connors, 1989).

The most common firing pattern for interneurons is “fast spiking” (Bacci et al., 2002), (Beierlein, Gibson & Connors, 2003). However, interneuronal firing patterns are heterogeneous, so their classification is rather complicated (Markram et al., 2004). Such heterogeneity of firing patterns may be relevant in light of the recent classification based on cluster analysis (see above) where the intrinsic electric excitability is related to morphological features. On the other hand, the regular spiking pattern is a constant and easily recognizable feature of excitatory neurons.

In this dissertation, while we will describe the morphology of a limited number of sampled cells, we will use the “electric signature” of regular spiking cells as a hallmark of glutamatergic neurons and as a criterion for selection throughout all of our experiments. This quick approach allows for the identification of samples at the beginning of each experiment, a great advantage in functional studies. Some morphological features, such as the shape of cell somata and the morphology of proximal dendrites, are also useful clues for patch targeting in fresh preparations.

Neurotransmitters in the barrel cortex

Most of the brain cortex neurotransmission relies on glutamate and GABA. These two neurotransmitters regulate the excitatory/inhibitory balance of cortical activity. Synaptic glutamate activates AMPA/kainate and NMDA receptors induce a cationic-based neuronal depolarization. Glutamate is effectively excitatory during the embryonic age, but, at early stages of development, the brain’s functional connectivity is low. In the first weeks, the spreading of second messengers such as inositol 1-3 triphosphate (IP3) and Ca^{2+} waves through gap-junctions (see below) is an effective excitatory mechanism for neuronal communication (Rorig &

Sutor, 1996). Neuronal coupling is mostly lost through development. At the same time, the number of chemical synapses and functional contacts increases so that chemical neurotransmission can take over. The development of GABAergic neurotransmission is more complicated. GABA activates two types of receptors: $GABA_A$ receptors ($GABA_AR$), which are chloride channels, and $GABA_B$ receptors ($GABA_BR$), which are G-protein coupled receptors. Part of $GABA_A$ mediated effects are excitatory rather than inhibitory until the end of the first postnatal week (Khirug et al., 2005) (Rivera, Voipio & Kaila, 2005). The reason for this is the high chloride concentration inside neurons, which, at an early age, is comparable to its concentration in the extracellular interstitia. Later, the developmental upregulation of the neuronal chloride transporter (KCC2) reduces the chloride concentration in the cytosol (Uvarov et al., 2007), (Zhu, Lovinger & Delpire, 2005). Thus, the flux of chloride through $GABA_AR$ becomes hyperpolarizing, and $GABA_ARs$ achieve their mature inhibitory function. At postnatal day 8 (P8) $GABA_ARs$ activation has already become inhibitory (Kobayashi et al., 2008), (Uvarov et al., 2007). This was the age of the animals, referred to in this dissertation. $GABA_BRs$ are G-protein coupled receptors that modulate voltage-gated ionic channels. Their activation can either boost potassium conductance (Koyrakh et al., 2005) or reduce Ca^{2+} (presynaptic) currents. In both situations, such receptors promote neuronal inhibition. This happens either through cell membrane hyperpolarization or through the decrease of synaptic vesicle release. $GABA_BRs$ are not subjected to developmental switches like the one occurring to $GABA_ARs$; they are therefore effectively inhibitory during the embryonic age.

Coupling and development

Coupling occurs between several types of cells in the mouse cortex at an early age. During an early postnatal period, neurons are widely coupled (Peinado, Yuste & Katz, 1993), (Roerig & Feller, 2000). Neuronal coupling drastically decreases within a few weeks, but it persists between interneurons until early adulthood (Priest, Thompson & Keller, 2001). Oligodendrocytes are the myelinating cells of the central nervous system. A description of these cells is irrelevant for the purposes of present dissertation. It is important to mention, however, that homologous and heterogous coupling occurs between oligodendrocytes and astrocytes in different brain regions (Maglione et al., 2010). This was documented with *in situ* dialysis and immunolabeling. Interestingly, heterologous coupling emerged only when the dialysis started from oligodendrocytes and depended on connexin 47. Astrocytes are widely coupled throughout developmental stages and will be described in detail next.

Astrocytes

Astrocytes are the major type of glial cell in the central nervous system.

These cells function as the brain's connective tissue but also provide trophic and metabolic support for neurons, regulate synaptogenesis and development, (Kettenmann & B.R., 2004) and control the extracellular concentration of ions and neuroactive substances (Schousboe, 2003), (Huang & Bergles, 2004), (Seifert, Schilling & Steinhauser, 2006), (Wallraff et al., 2006)

Astrocytes have low membrane resistance and an ohmic current-voltage relationship. They are endowed with ion channels, although their expression level

is low and does not efficiently support active electrical behavior as in neurons (Orkand, Nicholls & Kuffler, 1966), (Sontheimer, 1994), (Verkhratsky & Steinhauser, 2000), (Seifert & Steinhauser, 2001). On the other hand, astrocytes are excitable cells: the cytosolic variation of calcium concentration is the typical pathway of signal transduction on which astrocytic excitability is based (Cornell-Bell et al. 1990, Charles et al. 1991), (Cornell-Bell et al., 1990), (Charles et al., 1991). Calcium-based excitability is the main mechanism by which astrocytes respond to neuronal activity (Grosche et al., 1999), (Kulik et al., 1999), (Matyash et al., 2001), (Porter & McCarthy, 1996), (Pasti et al., 1997), (Bezzi et al., 1998), (Kang et al. 1998), (Araque et al., 2002), (Hirase et al., 2004), Wang et al. 2006) (Dombeck et al., 2007), (Gobel, Kampa & Helmchen, 2007), (Bekar, He & Nedergaard, 2008), (Schummers, Yu & Sur, 2008), (Perea & Araque, 2005), (Peters et al., 2003), (Schipke et al. 2008), although calcium transients in these cells can also occur spontaneously (Hirase et al., 2004), (Takata & Hirase, 2008) (Nimmerjahn et al., 2004). Mechanisms through which astrocytes can sense neuronal activity are multiple as these glial cells possess receptors for glutamate (Verkhratsky, Orkand & Kettenmann, 1998), (Seifert & Steinhauser, 1995), (Lalo et al., 2006), (Lalo et al., 2008), (Luque & Richards, 1995), (Mathyas et al. 2001), GABA, glycine, (Bowman & Kimelberg, 1984), (Kettenmann, Backus & Schachner, 1984) and a variety of metabotropic receptors (Verkhratsky & Kettenmann, 1996), (Verkhratsky, 2006), (Verkhratsky et al., 1998). Metabotropic receptors are the primary trigger of calcium-based astrocytic excitability as they are coupled to G proteins that in turn stimulate phospholipase C leading to the formation of inositol triphosphate (IP3) and calcium release from intracellular

stores (Pasti et al., 1997), (Porter & McCarthy, 1997), (Bezzi et al., 1998), (Kang et al 1998), (Kulik et al., 1999), (Araque et al., 2002), (Deitmer & Rose, 2010).

Ca^{2+}-mediated pathways trigger the release of modulatory substances. In such a way, astrocytes are capable of shaping neuronal communication and plasticity (Araque & Perea, 2004), (Volterra & Steinhauser, 2004), (Allen & Barres, 2005). Such process, known as gliotransmission, will be described later in more detail.

Astrocytes owe their name to the star-like pattern in their branching which results in widespread, non-overlapping domains covering virtually all of the brain's interstitial surface (Nedergaard, Ransom & Goldman, 2003). A single astrocyte in its domain contacts up to hundreds of thousands of synapses integrating their function in a so-called "tripartite synapse" (Deitmer & Steinhauser, 2010), (Halassa et al., 2010). Astrocytes form syncytia. They are indeed widely coupled through gap-junctions (Latour et al., 2001) which are mainly formed by connexin 30 and 43 (Gosejacob et al., 2011), (Theis et al., 2003). Recent reports show that in barrel cortex astrocytes sincytia are organized in columns and their coupling is sparse across the barrel septa (Houades et al., 2008). Astrocytic coupling allows the diffusion of rather large molecules across neighboring cells. This feature has been used by previous researchers to systematically dialyze astrocytes with desired solutions. This is achieved with patch clamp experiments starting from a single cell held in whole-cell configuration (Serrano et al*,* 2006). This approach will be adopted as a conditioning paradigm in the course of our experiments. Astrocytes preserve their gap junctions even in adulthood, but, after development, the thinness and complexity of their processes forms an obstacle to the rapid diffusion of molecules between cells (Peters et al., 2009). The rate of coupling

between astrocytes varies according to each brain region, age and health conditions. The shape of local networks is likely to reflect physiological demands of each brain district and be altered by stress conditions (Matyash & Kettenmann, 2010), (Peters et al., 2009). Astrocyte somata and processes shrink to a small size during brain maturation. In adulthood they can reverse again to their “immature” morphology in the course of brain pathologies such as ischemia (Martin et al., 2007) or Alzheimer’s disease (Peters et al., 2009). In such conditions a pro-inflammatory reaction known as “reactive gliosis” affects astrocytic morphology, coupling and several physiological properties that regulate interactions between glia and neurons (Seifert, Carmignoto & Steinhauser, 2010), (Sidoryk-Wegrzynowicz et al., 2011).

Astrocytes are morphologically and physiologically very heterogeneous, but they all express the “glial fibrillary acidic protin” (GFAP) which is typically used as a cell-type marker. In a mouse line expressing eGFP under GFAP promoter, non-astrocytic astroglial cells were found labeled in green as the astrocytes (Matthias et al., 2003). These cells did not express AN2 (mouse equivalent to rat NG2) and represented an astroglial cell population on its own. In our experiments, the peculiar somatic profile identified these cells as non-astrocytes allowing their rejection when fortuitous targeting occurred. We found such cells, though rarely, in both animals where astroglia were marked by eGFP expression and in animals where astroglial cells were marked by dsRED. We did not study these cells in the course of our experiments.

Gliotransmitters and neuron-astrocyte interaction

Astrocytes sense the neuronal activity as described above; furthermore, they can modulate such activity through the release of neuroactive substances called gliotransmitters (Araque et al., 1998), (Araque et al., 2000), (Arcuino et al., 2002), (Beattie et al., 2002), (Koizumi et al., 2003), (Zhang et al., 2003), (Bezzi et al., 2004), (Fiacco & McCarthy, 2004), (Newman, 2004), (Pascual et al., 2005), (Kozlov et al*,* 2006), (Serrano et al*,* 2006), (Perea & Araque, 2007), (Navarrete & Araque, 2008), (Perea, Navarrete & Araque, 2009), (Lee et al*,* 2010), (Nedergaard, Rodriguez & Verkhratsky, 2010), (Halassa & Haydon, 2010) (Bergles, Jabs & Steinhauser, 2010).

A well-described gliotransmitter is glutamate. This amino acid is released by glial cells through multiple mechanisms. One involves the Ca^{2+}-mediated fusion of synaptic vesicles similarly to what happens for the glutamate release pathway in the neuronal synapses (Parpura et al., 1994). Other pathways involve the reversal uptake of glutamate transporters (Szatkowski, Barbour & Attwell, 1990), anion-channel-mediated glutamate efflux (Kimelberg et al., 1990), diffusion through purinergic receptors (Duan et al., 2003), hemichannels (Ye et al., 2003) and glutamate release through the glutamate/cystine antiporter (Warr, Takahashi & Attwell, 1999). Some authors reported that glutamate release mediates slow inward currents in neurons (Fellin et al., 2004), (Navarrete & Araque, 2008). Others (Kang et al., 1998), (Liu et al., 2004) showed that some forms of glutamatergic gliotransmission depending on astrocytic Ca^{2+} elevation can potentiate or depress the activity of inhibitory synapses. Specifically, $GABA_BRs$ stimulation on the astrocytic membrane caused the elevation of their intracellular

Ca^{2+} (Kang et al., 1998). This in turn potentiated the inhibitory neurotransmission in a mechanism involving the downstream AMPA receptors at the neuronal synapses. Similarly, the astrocytic Ca^{2+} elevation was shown to mediate the release of glutamate (Liu et al., 2004). In this latter study, however, the gliotransmitter activated some neuronal glutamate metabotropic receptors (mGluRs). mGluRs activation decreased the amplitude of evoked inhibitory postsynaptic currents and the frequency of inhibitory spontaneous currents. The same gliotransmitter could therefore mediate opposite neuromodulatory effects due to the presence of different receptors on the neuronal membranes.

D-serine is an important gliotransmitter co-released by astrocytes together with glutamate (Mothet et al., 2005). This amino acid is a potent glutamate coagonist binding on the “glycine syte” of the NMDA receptors. Hennenberger et al. (2010) found that D-serine is necessary for long term potentiation (LTP) in hippocampus. In this study, the conditioning protocol for LTP induction also caused the Ca^{2+} elevation in neighboring astrocytes. The impairment of astrocytic Ca^{2+} elevation prevented the release of D-serine and, in turn, the occurrence of LTP.

Ca^{2+} elevation also mediates the astrocytic release of ATP (Guthrie et al., 1999), (Cotrina et al., 2000), (Newman, 2001). ATP has autocrine effects on astrocytic Ca^{2+} waves and paracrine effects on neurons. The most heterogeneous effects of ATP in the brain are due to the multiplicity of its derivatives and to the variety of its receptors (Burnstock, Fredholm & Verkhratsky, 2011). ATP release from astrocytes, for instance, modulates the brainstem neuronal activity controlling the respiratory rhythm (Gourine et al., 2010). In extracellular space, on the other hand, ATP is quickly converted into adenosine by ectonucleotidases (Gallagher &

Salter, 2003), (Fam et al., 2003). A1 adenosine receptors mediate presynaptic neuronal inhibition (Pascual et al., 2005), which induces, for instance, the heterosynaptic depression between hippocampal neurons (Serrano et al., 2006). Heterosynaptic depression depends on astrocytic Ca^{2+} elevation upon $GABA_B$ receptors activation. The mechanism is suggested to prevent network saturation or to decrease the signal to noise ratio between the principal synapses and those not primarily recruited by a certain stream of information. Another role for astrocytic adenosine is the control of sleep. Ambient adenosine concentrations affect perceived drowsiness and cognitive abilities (Halassa et al., 2007), (Halassa et al., 2010). In heterosynaptic depression, one of the roles of tonic adenosine fluctuation could be the prevention of synaptic saturation.

GABA secretion from astrocytes is also described in literature (Angulo et al., 2008) (Koch & Magnusson, 2009) and, in several circumstances, it proved to be Ca^{2+} dependent (Verderio et al., 2001), (Kozlov et al., 2006), (Lee et al., 2010). Not many studies provide information about the molecular pathway of such mechanism or about its physiological relevance. The first functional evidence of GABA release from astrocytes was provided in 2006 (Kozlov et al., 2006). In such study Ca^{2+} rise in astrocytes was evoked by mechanical stimulation. This caused the release of GABA, measurable in the electric currents from neighboring neurons. Such currents had slow kinetics, large amplitudes and were stochastic. They occurred also in unstimulated tissue, but their event frequency was very low and increased upon astrocytic stimulation and from astrocytic Ca^{2+} elevation. The authors couldn't identify the possible molecular pathway mediating such type of gliotransmission. The first experiments providing a molecular mechanism for

astrocytic GABA release are very recent (Lee et al., 2010). In this study, GABA was released from the Bergmann glia (cerebellar astrocytes) and accounted for the tonic inhibition of cerebellar neurons. The mechanism was mediated by the opening of a Ca^{2+}-gated chloride channel (Bestrophin). GABA could be released through Bestrophin upon Ca^{2+} elevation due to the large size of the channel's pore. Furthermore, it was recently shown by Andersson and Hanse (2010) that a burst of neuronal activity in the adult hippocampus induces a transient period of "postburst depression." Such transient depression lasted approximately one second and depended on Ca^{2+} elevation in astrocytes. No downstream pathway of gliotransmission was indicated by the authors.

Additionally, astrocytic release of gliotransmitters modulates neurotransmission in other physiological contexts such as epilepsy (Kumaria, Tolias & Burnstock, 2008), (Seifert et al., 2010), (Gomez-Gonzalo et al., 2010), gating of pain perception (Bardoni et al., 2010), and network depression induced by hypoxia (Martin et al., 2007). In some of these circumstances, Ca^{2+} elevation could be detrimental and determine excitotoxicity. Pharmacologically evoked seizures, for instance, were worsened by astrocytic Ca^{2+}-mediated gliotransmission in a sort of excitatory loop of glutamate release involving positive feedback between astrocytes and neurons (Gomez-Gonzalo et al., 2010).

In contrast to the aforementioned bibliography, recent experiments challenged the entire concept of Ca^{2+}-mediated gliotransmission. Mutant mice have been generated to selectively increase or obliterate astrocytic Ca^{2+} signalling by alteration of G-protein-related pathways. Surprisingly, in either of these manipulations, astrocytes failed to modulate the neuronal activity (Fiacco et al.,

2007), (Petravicz, Fiacco & McCarthy, 2008), (Agulhon, Fiacco & McCarthy, 2010). Despite such disagreement, some options, mainly concerning different methodologies, are considered as a possible source of such discrepancies (Kirchhoff, 2010). In this regard, it was pointed out that the mechanisms of gliotransmission might be Ca^{2+}-dependent but involve other mediators rather than G-protein coupled receptors on astrocytes. An interesting publication in this perspective indicates an alternative mechanism of astrocytic Ca^{2+} elevation (Shigetomi et al., 2010). In such work it has been found that Ca^{2+} transient can occur in microdomains close to the plasma membrane and in the astrocytic distal processes. Such fast Ca^{2+} transients are largely missed by conventional Ca^{2+} sensors but are detected by the innovative membrane-targeting sensor used by the authors. Such microdomains might be independent from G-protein receptors and rely on other local triggers. It is tempting to speculate that this could account for part of the gliotransmission mechanisms described so far. In addition, the microdomain activity is abolished with BAPTA dialysis of the astrocytes, a methodology adopted by several researchers to investigate gliotransmission (e.g. Serrano et al*,* 2006, Hennenberger et al*,* 2009).

Aim of the study

In vivo experiments (Wang et al., 2006) showed that mouse whisker stimulation evokes calcium responses of astrocytes in the barrel cortex. In acute slices (*in situ*), in the same brain region, it was shown that such responses were restricted to the stimulated sensory column and depended upon the activation of layer 4 neurons (Schipke, et al., 2008). Astrocytic responses evoked by neuronal activity suggested the presence of a functional interaction which might be relevant in the

barrel cortex for processing incoming sensory inputs. Yet, to date, gliotransmission in this brain region has not been thoughtfully studied.

The aim of the present study is to investigate with physiological methods the pathways by which astrocytes can modulate neuronal activity in the barrel cortex and, in particular, understand the role of astrocytic intracellular calcium in gliotransmission and neuromodulation. To that end, the barrel columns will be stimulated *in situ* and the astrocytic and neuronal activity will be measured with calcium imaging and whole-cell patch clamp techniques respectively. To understand the role of astrocytic calcium signaling and its potential involvement in gliotransmission, selective chelation of intracellular calcium with BAPTA will be applied. Pharmacological inhibitors will be employed to characterize the contribution of different neurotransmitter/gliotransmitter receptors. With all these experiments, the present work shows that calcium-dependent gliotransmission accounts for the reinforcement of GABAergic inhibition in the barrel neurons. Potential pathways of gliotransmission, such as purine, serine, or glutamate transmission, are only minimally involved or not involved at all.

Astrocytic-mediated GABAergic inhibition of barrel cortex neurons limits the extent of their widespread and synchronous depolarization.

MATERIALS AND METHODS

Ethical approval

Transgenic animals were bred in the local animal facilities and handled for experiments according to the guidelines of Directive 2010/63/EU of the European Parliament for the protection of animals used for scientific purposes and the Federal Ministry of Health or “Landesamt für Gesundheit und Sozialen” (LaGeSo).

Animal preparation and Ca^{2+} imaging

Acute brain slices were prepared from eight to 10-day-old NMRI mice (Charles River, Germany) or from the transgenic mouse lines eGFP/GFAP (Nolte et al., 2001) and mRFP1/GFAP (Hirrlinger et al., 2005), (kindly provided by Prof. F. Kirchhoff). Transgenic animals expressed enhanced green fluorescent protein (eGFP) or red fluorescent protein (mRFP1) under the control of the human glial fibrillary acidic protein (GFAP) promoter after animal decapitation slices of 250 µM thickness were prepared following the protocol by Agmon and Connors (1991). Before recording, slices were incubated for at least 30-45 minutes in artificial cerebro spinal fluid (ACSF) at room temperature. For Ca^{2+} imaging, slices were loaded with Fluo-4-AM as described in Peters et al. (2003) (Peters et al., 2003). Imaging and patch clamp experiments were performed with an upright Zeiss microscope. During the experiments slices were kept in a perfusion chamber at 32-34°C with constant ACSF flow of about 5 ml/min. Barrel fields were identified in bright field illumination (Schipke, Haas & Kettenmann, 2008). Local barrel stimulation was applied through a glass electrode (tip opening about 20 µm)

placed in layer 4 of the cortex within a given barrel field. The stimulus consisted of 30 voltage pulses at 30 µA, duration of a single stimulus 1 ms, 100 Hz stimulation frequency (Schipke et al., 2008). The stimulation protocol as well as the patch clamp recording was performed with a patch clamp amplifier (EPC 9 or EPC9/2, HEKA Elektronik, Lambrecht, Germany) and traces were acquired with a 3.0 KHz Bessel filter. For stimulation, the amplifier voltage output was connected to an external stimulus isolator (NeuroLog, NL 800, Digimaster Ltd, Hertfordshire, UK). Images for Ca^{2+} measurements were acquired at 1Hz, 300 ms exposure time. Patch clamp acquisitions and imaging experiments were performed with three softwares: TIDA (HEKA Elektronik, Lambrecht, Germany), Imaging Cells Easily (ICE, own development) or Camware (PCO Imaging, Kelheim, Germany).

Immunohistochemistry and morphological characterization

After biocytin dialysis of single neurons, slices were fixed overnight in phosphate buffered solution (PB) 0.1 M and 4% paraformaldehyde. Biocytin-filled neurons were then marked with streptavidin conjugated to CY3 (1:200, Covance/HISS Diagnostic GmbH, Freiburg, Germany). After fixation slices were incubated in a solution containing 0.2% Triton X-100, 2% BSA and 10% normal goat serum (NGS) in phosphate buffer at pH 7.4 for 4h to permeabilize and block non-specific binding. Cy3-conjugated streptavidin was diluted in 0.1M phosphate buffer containing 0,2% TX-100, 2% BSA, 5%NGS. In some experiments (data not shown), DAB-peroxidase staining was used as alternative to immunofluorescent staining. Image stacks were acquired with a confocal microscope (SPE, Leica Microsystems, Germany) and maximal intensity projections were reconstructed

with Image J software (Rasband, W.S., ImageJ, U. S. National Institutes of Health, Bethesda, Maryland, USA, http://rsb.info.nih.gov/ij/, 1997-2009).

Solutions and drugs

Standard ACSF contained in [mM]: NaCl [134], KCl [2,5], $CaCl_2$ [2], $MgCl_2$ [1.3], K_2PO_4 [1.25] (Merck KGaA, Darmstadt, Germany), glucose [9] and $NaHCO_3$ [26] (for storing at room temperature prior to experiment) or [21.4] (in the recording chamber at 32-34°C). Pipette solutions for neurons contained in [mM]: K-gluconate [120], KCl [10], $MgCl_2$ [1] ethylene glycol tetraacetic acid (EGTA, Sigma) [0.1] $CaCl_2$ [0.025] HEPES [10] $ATPK_2$ [1], (Sigma) GTPNa [0.2] (Amersham Biosciences, Piscataway, NJ, USA) glucose [4], (Kang et al. 1998) (Kang et al., 1998). In the pipette solution with high [Cl^-], K-gluconate was substituted with KCl (pH 7.2). The pipette solution for astrocytes contained in [mM]: K-gluconate [90], 1,2-bis (o-aminophenoxy) ethane-N,N,N',N'-tetraacetic acid (BAPTA, Sigma) [40], $MgCl_2$ [1], NaCl [8], ATP [2], GTP [0.4], HEPES [10] (pH 7.2) and in the control dialysis experiments BAPTA was substituted by K-gluconate (Serrano et al., 2006). Sulforhodamine (Sigma) was added in concentration of 0.1 mg/ml, Fluo 4-AM (Invitrogen) at 10 μM and membrane impermeable Fluo 4 (Invitrogen GmbH, Darmstadt Germany) was added at 20 μM to the pipette solution. Drugs were applied at the following concentrations in [μM]: baclofen [20] (Tocris) CNQX [20] (Sigma), LY367385 [200] (Tocris, Ellisville, Missouri, USA), MPEP [100] (Tocris), gabazine [10] (Tocris), CGP55845 [5] (Tocris), CPT [4] (Sigma), MK801 [10] (Sigma), strychnine [5] (Sigma) *trans*-ACPD [100] (Sigma). Drugs were preincubated for one to two minutes before stimulation. D-AAO was used at the concentration of 17 U/ml. For D-AAO

experiments, the brain slices were preincubated (30 to 90 minutes) at room temperature in oxygenated ACSF in which the enzyme was dissolved. The final concentration of DMSO (Sigma), in which some drugs were dissolved, was tested alone and proved to have no effect on the neuronal evoked response. Intra and extracellular solution components, where not otherwise stated, were produced by Carl Roth GmbH, Karlsruhe, Germany.

Data analysis

For analysis of electrophysiological data and statistical analysis we used TIDA (HEKA Elektronik, Lambrecht, Germany), Origin (OriginLab, USA), Microsoft Excel and Image-Pro PLUS 5.1 (Media Cybernetics, Inc. MD, USA). Data are shown as mean (± SEM); significance was determined with the appropriate T-test or with Anova-One-way test. APs half width and frequency were analyzed with a custom made function of the software IGORpro written and kindly provided by Dr. K. van Aerde and Prof. D. Feldmeyer, (Forschungzentrum, Juelich); the AP threshold was determined according to Kole and Stuart (2008) (Kole & Stuart, 2008). The stimulus-evoked depolarization in neurons was measured at time points when no AP occurred. The integral of stimulus-evoked depolarization over time (ISTM) was determined from the baseline at the resting voltage and also included the time course of APs. Fluo-4 fluorescence recordings were normalized (F/F0) and filtered using a median filter. F0 was obtained by averaging 10 frames at the beginning of the recording. To determine the area occupied by Ca^{2+}-responsive astrocytes, we compared images prior to stimulation and between and one to three seconds after stimulation. The area was composed of pixels which increased in brightness above threshold. Lateral drift of the imaged field induced

by movements of the sample during the experiment was manually corrected. Ca^{2+} kinetics were analyzed with Image Pro (Media Cybernetics, Inc. MD, USA).

RESULTS

Morphological and physiological properties of selected neurons

Neurons in the brain cortex, as described above, are a heterogeneous population of excitatory and inhibitory cells. They have characteristic morphologies and electrophysiological features. We decided to determine which category was mostly targeted in our patch clamp experiments. Without other criteria for selection, we patched cells with round small somata within layer 4 (L4) and cells with triangular somata in layer 2/3 (L2/3). With current clamp experiments, we measured their AP spiking properties. To evoke AP firing, we delivered depolarizing current in steps of increasing intensity (step size: 10 pA, step duration: 500 ms). We determined the AP frequency in relation to the amplitude of injected current. The maximal AP frequency was typically observed at about -20 mV (100 pA current injection), namely 105 Hz ± 8 Hz for neurons in L2/3 (N = 17) and 96 Hz ± 10Hz in L4 (N = 15) (Fig.1.a). Comparing L4 and L2/3, no significant differences between neuronal firing frequencies were observed (P = 0.4). AP half-width was 2.9 ± 0.2 ms in L2/3 neurons and 2.1 ± 0.2 ms in L4. We frequently observed firing adaptation as previously described for excitatory neurons (Agmon & Connors, 1992). These characteristics are typical for “regular-spiking cells” such as spiny-stellate and pyramidal neurons (Agmon & Connors, 1992). We also analyzed neuronal morphologies with the confocal microscope after single-cell dialysis with biocytin, tissue fixation and labeling with fluorescently tagged streptavidin. After morphological reconstruction, most cells observed in L4 (N = 7 of 8) were spiny stellate neurons (Fig.1.b1), with star-like branching dendrites,

occasional asymmetry toward the center of the barrel, round cell somas and columnar axonal projections often extending to the white matter.

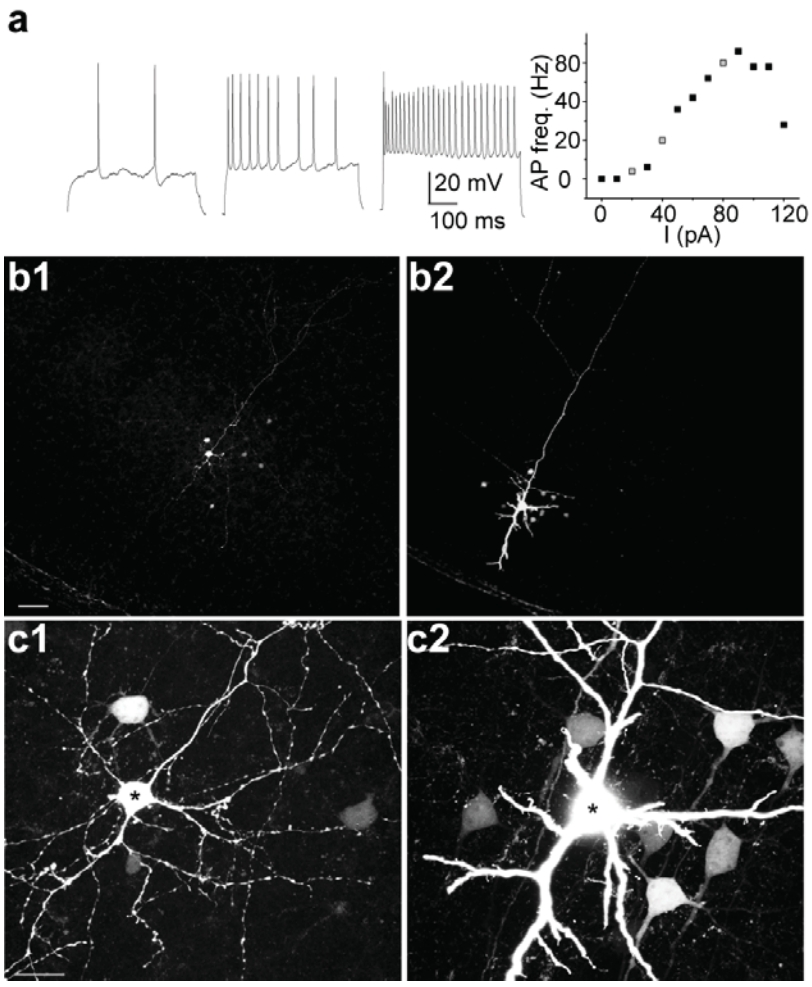

Fig.1 *Selected neurons had physiological and morphological features of spiny stellate and pyramidal cells. a. Three sample traces show AP firing at increasing frequencies (left). Scatter-plot describes the relation between the amplitude of injected current and the frequency of APs (right). Dots in grey are the data points corresponding to the three samples shown on the left. Cells were depolarized for 500 ms with increasing current steps (step size: 10 pA). b. L4 (b1) and L2/3 (b2) neurons dialyzed with biocytin through the patch pipette. Scale bar 150 µm c. Same cells as in b at higher magnification (scale bar 20 µm). Note the coupled cells in L4 (c1) and L2/3 (c2). Asterisks mark the patched cell.*

In L2/3, most cells (N = 12 of 13) had a typical “pyramidal neuron” morphology (Fig.1.b2): thick apical dendrites directed toward the pial surface, triangular somata and columnar axonal projections toward the white matter (White & Rock,

1980), (Lubke *et al.*, 2000). Two neurons in L4 and L2/3 could not be unequivocally identified by their morphology, however their firing pattern was that of “regular spiking” (data not shown). We concluded that morphological and physiological criteria classify these cells as excitatory neurons.

Neuronal coupling

We found a remarkable amount of coupling (Fig.1.c and Fig.2) between spiny stellate cells in L4 (5 out of 8 experiments, Fig.1.c1) and pyramidal cells in L2/3 (7 out of 13 experiments Fig.1.c2).

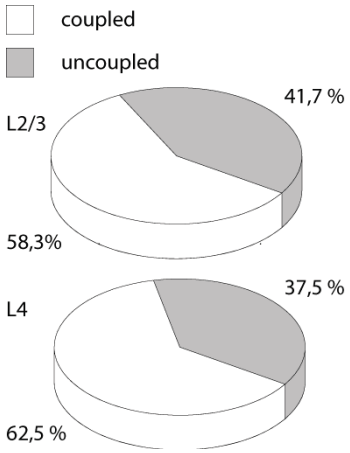

Fig.2 *Neurons in L2/3 (upper chart) and in L4 (lower chart) are coupled through gap junctions. Pie charts show the percentage of cells that, upon dialysis, showed dye-coupling (white chart areas) and those that were uncoupled (gray chart areas).*

This was unexpected since coupling between spiny stellate cells has not yet been reported, while coupling between pyramidal cells, has already been described during development (Peinado et al., 1993). We determined the coupling probability as a percentage of experiments in which at least two neurons were dye-coupled (five out of eight experiments in L4 and seven out of 13 experiments in L2/3). Based on these criteria the coupling probability was 58.3% in L2/3 and 62.5% in L4 (Fig.2).

Evoked response in and outside the stimulated column

The local electric stimulation of L4 delivered through an electrode as a train of electric spikes (300 Hz, 30 μA) induced a rapid neuronal Ca^{2+} increase (not shown). This was followed by a slower astrocytic Ca^{2+} increase within the stimulated somatosensory column (Fig.3.a). These responses have been characterized with Ca^{2+}-imaging experiments in previous publications (Schipke et al, 2008). In the present work, we focused rather on the neuronal response, measured as whole-cell current with patch clamp recordings. We still used Ca^{2+} imaging to quantify the extent of astrocytic response in some experiments. We observed that upon stimulation virtually all neurons within a given barrel incurred in a synchronous depolarization (Fig.3.b1, *in*). We chose three parameters to analytically describe such stimulus-evoked response: 1) the average amount of cell depolarization (inter-spike baseline) during the electric stimulation (STM depol), 2) the half-decay time from STM depol to membrane-potential baseline (Half rep) and 3) the integral under the evoked response within four seconds after STM depol (ISTM). Inside the stimulated barrel (Fig.3.b1 *in,* and 3.c) STM depol was 30 ± 1 mV from a holding potential at -68.7 mV ± 0.3 mV (N = 92). During the period of stimulation (STM) neurons typically fired a burst of APs (Fig.3.b1, *in*). After STM the membrane repolarized and Half rep was 0.6 ± 0.03 s. ISTM was 26.9 ± 1.5 mV*s. The neuronal evoked response within the stimulated barrel was largely removed by bath application of TTX (Fig. 3.b2, TTX) (N = 6). In such conditions, the average STM depol was decreased to 4.3 ± 1.4 mV (17% of internal control) and ISTM was equal to 4.4 ± 1.1 mV*s (24% of the internal control). No AP was fired during stimulation (Fig.3.b2). During TTX application,

the resting membrane potential almost instantly decreased to resting values; therefore, we didn't quantify Half rep in these experiments.

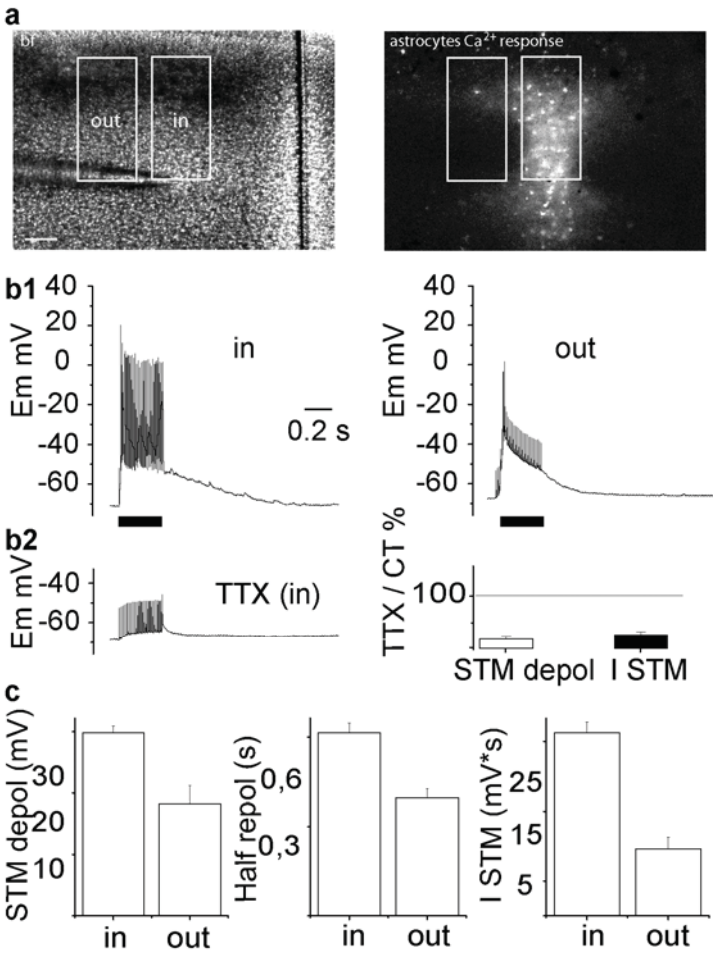

Fig.3 *The neuronal stimulus-evoked response is significantly smaller outside the stimulated barrel. a. Barrel cortex: bright field image (left) and astrocytic response to electric stimulation: visible as a fluorescent signal in* Ca^{2+} *(*Ca^{2+}*) imaging (right). Note that the astrocytic response is mainly restricted to the stimulated barrel. Scale bar c.a. 150 µm. b1. Current clamp recordings: voltage traces (Em) of neuronal evoked response within (in) and outside (out) the stimulated barrel.* Black bars denote the period of stimulus delivery. *b2, left: Neuronal evoked response (in) is blocked by tetrodotoxin (TTX); b2 right: Bar graph shows the amplitude of evoked depolarization (STM depol) and the integral of membrane depolarization* (*ISTM) in the presence of TTX (normalized to control response previous to TTX application). c. Bar graphs: responses within (in) and outside (out) the stimulated barrel: amplitude of evoked depolarization (STM depol), time of half-repolarization (Half rep) and integral of evoked depolarization* (*I STM).*

We compared the neuronal recruitment within and outside the stimulated barrel (Fig.3.b1). “Outside” was essentially the adjacent somatosensory column: namely the region in closest proximity to the point of stimulation where astrocytic Ca^{2+} responses were not detected (N = 16, Fig. 3, a, b1). We observed that all the parameters of the neuronal evoked response were significantly smaller outside than within the stimulated barrel ($P < 10^{-3}$) (Fig.3.b1 and 3.c). Outside the stimulated barrel, STM depol was 18.3 ± 2.9 mV (Fig.3.c), Half rep was 0.40 ± 0.03 s and ISTM was 9.6 ± 1.7 mV*s. Moreover, during the stimulation, 95% of neurons within the stimulated barrel were induced to fire APs. Almost all of them (90%) fired a burst (more than one AP/response): during the evoked responses we quantified on average 15.8 ± 1.3 APs. In contrast, outside the stimulated barrel, only 62.5% of the neurons fired APs upon stimulation. Only 30% of them fired a burst: during the evoked responses we quantified on average 2.2 ± 0.9 APs.

These results show that within the zone of astrocytic Ca^{2+} response, neurons undergo large depolarization and fire synchronous bursts of APs during the stimulation. In nearby columns, the amount of membrane depolarization is smaller and the AP firing is reduced. Astrocytic Ca^{2+} increase within the stimulated barrel was shown to be a consequence of neuronal activity (Schipke et al. 2008) which we now characterized. Additionally, it appears that a weaker yet widespread activity outside the stimulated barrel is not sufficient to evoke astrocytic Ca^{2+} responses. There is, therefore, a minimum threshold of neuronal activity required for astrocytic recruitment.

In the subsequent part of the project, we focused exclusively on neuronal responses within the stimulated barrel: i.e. within the zone of astrocytic Ca^{2+} increase.

Ca^{2+} chelation in astrocytes

We hypothesize that astrocytes can modulate the neuronal evoked response and that this process depends on intracellular Ca^{2+} elevation. Therefore, the selective impairment of astrocytic Ca^{2+} should affect the neuronal evoked response. To test this, we dialyzed the astrocytes with a high concentration of Ca^{2+} chelator (BAPTA). BAPTA was dissolved in the patch-pipette solution and the dialysis started from a single astrocyte held in whole-cell configuration for 45 to 60 minutes. Due to the astrocytic gap-junctional coupling, our intracellular solution spread to neighboring cells as reported in previous publications (Serrano et al. 2006), (Andersson & Hanse, 2010). The following results in this paragraph are a validation of the procedure's efficiency. To identify astrocytes before dialysis, we used the mRFP1/GFAP mouse line where astrocytes were marked by the red fluorescent protein (mRFP1) expressed under the astrocytic promoter of glial fibrillary acidic protein (GFAP). Another mouse line with green-labeled astrocytes (eGFP/GFAP) was used for dye-coupling experiments. In such experiments, a red fluorescent dye (sulforhodamine B) was added to the pipette solution (Fig.4,a). In all experiments we dialyzed only positively identified astrocytes within L4 of the stimulated barrel (within 100 µm from the stimulation electrode). After establishing the whole-cell configuration, astrocytes displayed a negative membrane potential (c.a. -70 mV), low membrane resistance (in the range of 10 to 30 mΩ), and linear

voltage-current relation as described in previous publications (Serrano et al. 2006), (Schipke et al. 2008).

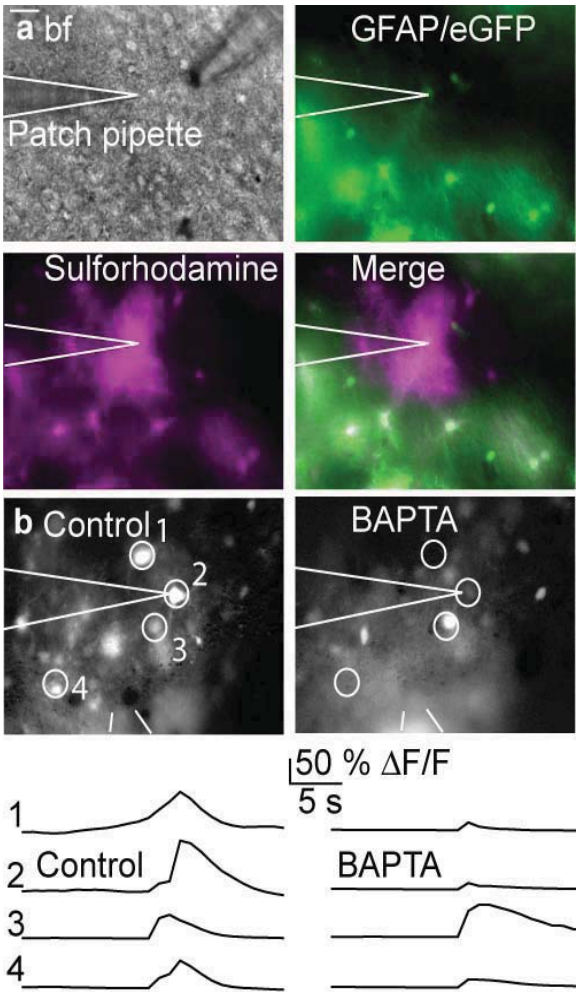

Fig.4 *Ca^{2+} is effectively chelated in astrocytes: a. Barrel Cortex. Up, right: Bright field image of L4 (bf). Up, left: same area, fluorescent astrocytes expressing enhanced green fluorescent protein (eGFP) under the Glial Fibrillary Acidic Protein promoter (GFAP). Down, left: fluorescence signal of Sulforhodamine-B (Magenta) after dialysis. From the patched cell, the dye spread into neighboring astrocytes. Down, right: merged image (Merge) of the astrocytic eGFP (green) and sulforhodamine-B fluorescence (magenta). b. Fluorescence of the Ca^{2+} indicator Fluo-4-AM in response to stimulation before (Control) and after 40-60 min of BAPTA dialysis (BAPTA). Traces at the bottom show the kinetics of response of the cells highlighted in the picture. Scale bar: 20 µm. Patch pipette position is outlined in white in each picture.*

In dye-coupling experiments we observed that after 45 to 60 min of dialysis, sulforhodamine B spread to 12 ± 2 cells (Fig.4.a; n = 6). In some experiments, we also added biocytin to the patch pipette. Dialysis was followed by slice fixation and DAB staining. After this procedure coupled cells were visible in black against the bright field of the microscope. In these conditions, we detected astrocytes

coupled in a wide syncytium (data not shown) similar to what was reported in Serrano et al. (2006). We then tested the efficiency of astrocytic dialysis with Ca^{2+}-imaging experiments. In these experiments, BAPTA dialysis reduced the Ca^{2+} response of astrocytes surrounding the patched cell. To quantify the extent of such effect, we selected a field of view of 4000 μm^2 at the microscope with the injected astrocyte approximately in the center. In this field, the amount of Ca^{2+} response occupied an area of 1600 ± 350 μm^2 in control conditions and 500 ± 200 μm^2 after BAPTA dialysis (typical response in Fig.4.b, N = 6). To exclude that the decreased Ca^{2+} response after dialysis was due to the Ca^{2+} sensor (Fluo-4-AM) washout, we added membrane-impermeable Fluo-4 to our pipette solution. We found that in these conditions the stimulation-evoked response decreased to 18.3 ± 2.4% of control (n= 12). Notably, even after BAPTA dialysis there were still a few astrocytes close to the patched one, in which the Ca^{2+} response was unaltered (Fig.4.b, sample 3). This suggests that the decrease in Ca^{2+} response after BAPTA dialysis is not due to mere sample bleaching. These data prove the effectiveness of whole-cell dialysis as a tool for selective and widespread Ca^{2+} chelation in the astrocytic syncytium.

BAPTA dialysis of astrocytes impaired their Ca^{2+} response locally but a large population of astrocytes was activated in a distal region

Barrel stimulation via extracellular electrode reliably triggers a Ca^{2+} increase in astrocytes within the stimulated somatosensory column (Schipke et al., 2008). The columnar geometry of such evoked response is a typical feature of the barrel cortex and a consequence of the local neuronal activity. In this brain area, a spreading of astrocytic response outside the stimulated column would predict an

increased neuronal excitability. Mindful of this, we studied the geometry of astrocytic evoked responses after local BAPTA dialysis. As described above, we locally impaired the astrocytic Ca^{2+} response dialyzing cells with BAPTA (Fig.5.a).

After 45 - 60 minutes of dialysis (N = 19) we observed a suppression of Ca^{2+} response up to ~200 μm from the patched cell (Fig.5.a, upper traces). Outside this region, however, astrocytes still responded to the stimulation with the usual Ca^{2+} rise (Fig.5.a, middle traces). Remarkably, outside the stimulated barrel (Fig.5.a, lower traces), particularly in L2/3 and L5, more cells responded to stimulation with a Ca^{2+} increase (N = 14). Therefore, after local BAPTA dialysis, the astrocytic Ca^{2+} response was no longer restricted to one column (Fig.5.a and 5.b). The response kinetic after dialysis was similar to the one seen within the barrel in control conditions (Fig.5.a, upper and lower traces). The area of astrocytic Ca^{2+} response was on average of 0.16 ± 0.04 mm^2 in control conditions (about 10 minutes before dialysis, Fig.5.c, “Control” white bar) and 0.35 ± 0.06 mm^2 after BAPTA dialysis (about 60 minutes after Control, Fig.5.c, “BAPTA” black bar) (P = 0.01).

In a separate set of experiments, omitting the procedure of BAPTA dialysis, we stimulated the barrel for two times at 60-minute intervals (N = 5). In such conditions, no significant difference (P = 0.9) was found between the areas of response. The response was 0.13 ± 0.04 mm^2 at the first stimulation (Fig.5.c, “Control1”) and 0.14 ± 0.04 mm^2 at the second (Fig.5.c, “Control2”).

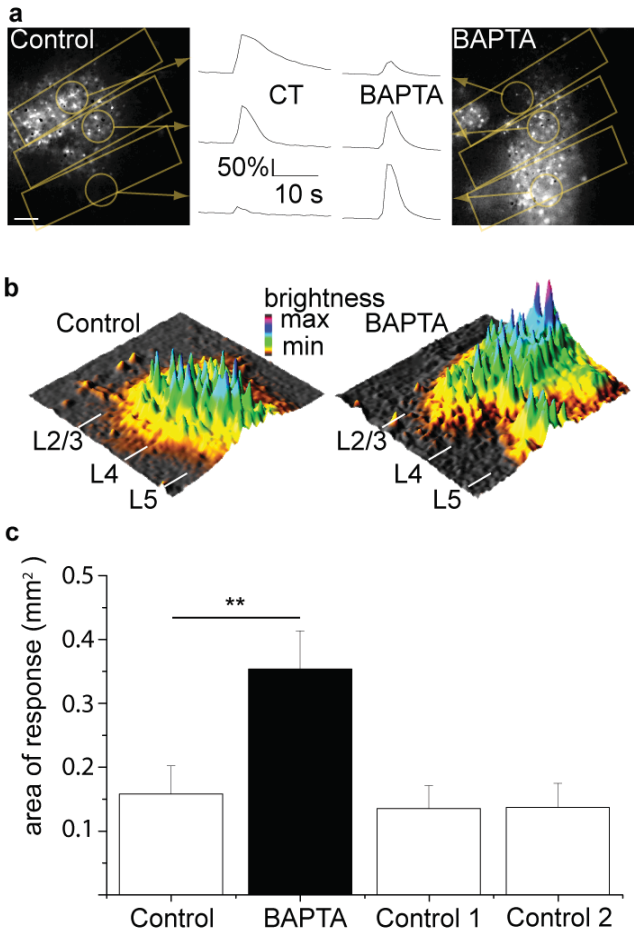

Fig.5 *BAPTA dialysis of astrocytes eliminated local Ca^{2+} response to stimulation but a larger population of astrocytes was activated in a distal region. a. Fluorescence images at the peak of the astrocytic evoked Ca^{2+} response: before (Control) and after dialysis of astrocytes with BAPTA. The borders of each barrel column are outlined in yellow. Regions of interest (ROI) are marked by yellow circles. Scale bar denotes 100 µm. Traces of fluorescence recordings from each corresponding ROI (pointed by arrows) are displayed in the middle. After BAPTA dialysis: in the upper ROI the Ca^{2+}-evoked response is suppressed; in the middle ROI the response is unaffected; in the lower ROI the response is increased due to newly recruited astrocytes. b. Spatial distribution of response from the figures in "a" with color-coded measurement of brightness ranging from min (dark gray) to max (magenta). c. Average area covered by responding astrocytes before (Control) and after 45 to 60 min BAPTA dialysis (± SEM). We repeated these experiments omitting the procedure of BAPTA dialysis: area of control-evoked response (Control1) and evoked response after 60 minutes (Control2). Two asterisks; P = 0.01 (one-way Anova).*

Astrocytic Ca^{2+} chelation leads to an enhanced neuronal evoked response

As described above, local astrocytic dialysis increased the astrocytic Ca^{2+} response outside the stimulated barrel. This strongly suggests an increased neuronal excitability. We therefore studied the neuronal evoked response in these conditions with current clamp experiments.

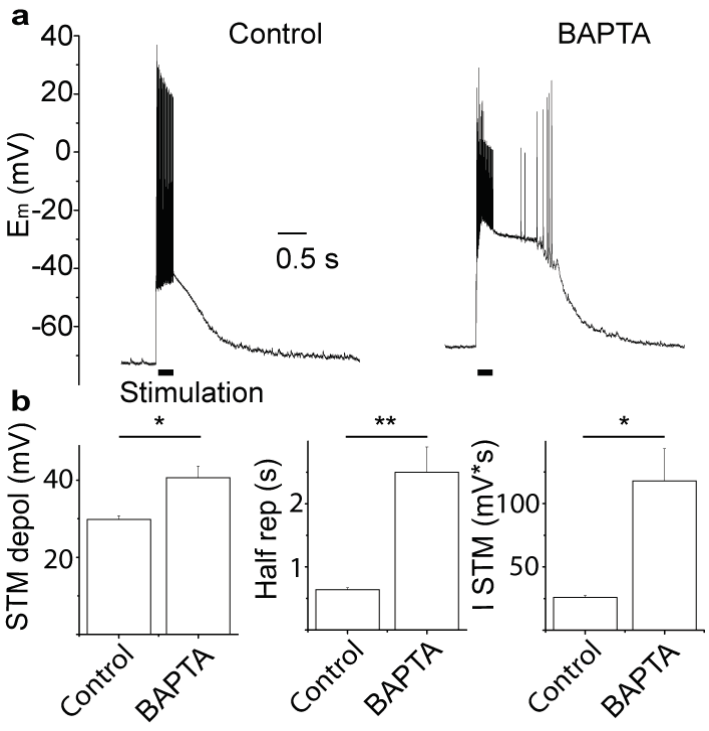

Fig.6 *Astrocytic Ca^{2+} chelation causes an enhanced stimulus (STM)-evoked response in neurons. a. Membrane potential (E_m) recording from a neuron within the stimulated barrel. STM-evoked neuronal response before (Control, left) and after dialysis of nearby astrocytes with BAPTA (right). The stimulation is indicated by a bar. b. Amplitude of the STM-evoked depolarization (left, STM depol); time of half-repolarization (middle, "half rep"); integral of the voltage trace (ISTM) during the evoked depolarization (right). Asterisk, P = 0,002; two asterisks P < 0.001 (unpaired T test).*

As shown in Fig.3 and Fig.6 (a, left), the stimulation in control conditions evoked sustained depolarization of the barrel neurons (30 ± 1 mV) (N = 92; Fig.6.a, left). After this, their membrane repolarized (0.6 s ± 0.03 s) to resting potential (-68.7 mV ± 0.3 mV). APs were superimposed on the neuronal depolarization during

stimulation but were rarely observed during the repolarization phase (< 5% of cells, data not shown).

When the stimulation was applied after astrocytic dialysis with BAPTA, we observed a larger and longer neuronal depolarization (N = 18; Fig.6.a, right). After astrocytic dialysis with BAPTA the STM depol in neurons was increased (P = 0.002) to 41 ± 3 mV and the Half rep was prolonged (P = 0.0003) to 2.5 ± 0.4 s due to an additional plateau phase. Moreover, in 9 out of 18 of these experiments we observed 1 to 16 (average 4.2 ± 1.4) APs during the repolarization phase. ISTM was on average 118 ± 25 mV*s (Fig.6, b) thus significantly increased (P = 0.002) in comparison to control conditions (26.9 ± 1.5 mV*s).

In some experiments, K-gluconate was added to the pipette solution for astrocytic dialysis instead of BAPTA, as a dialysis control (Fig.7). After c.a. 60 min of astrocytic dialysis with K-gluconate the neuronal response to stimulation was not significantly different from control (N = 12). STM depol was 24.14 ± 1.8 mV (P = 0.07), the Half rep was 0.67 ± 0.03 s (P = 0.53) and ISTM was 21.4 ± 1.9 mV*s (P = 0.27).

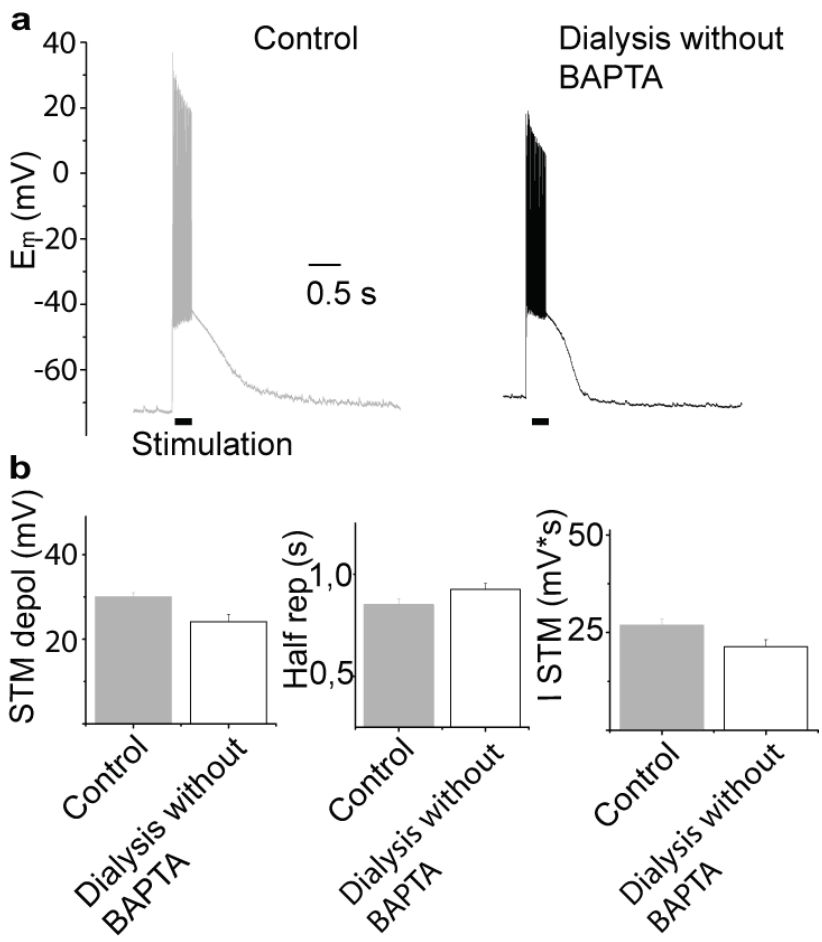

Fig.7 *Astrocytic dialysis with K-gluconate did not affect the evoked response in neurons. a. Typical membrane potential (E_m) recording from a neuron within the stimulated barrel. Evoked neuronal response before (Control, gray) and after dialysis with K-gluconate (Dialysis without BAPTA, black). The stimulation is indicated by a bar. b. Mean amplitude of the evoked depolarization (STM depol), time for half repolarization (Half rep) and integral of the voltage trace (ISTM) during the evoked depolarization. The parts highlighted in gray are the same as Fig.6 which are referred as "Control".*

Activation of $GABA_A$ and $GABA_B$ receptors inhibits neuronal evoked response

BAPTA dialysis of astrocytes caused an increased neuronal response (Fig.6) and a widespread astrocytic Ca^{2+} response (Fig.5). We therefore studied potential pathways that could account for an increased neuronal excitability after astrocytic BAPTA dialysis. GABAergic inhibition can be potentiated by astrocytic Ca^{2+} increase (Kang et al. 1998). GABAergic inhibition is also a prominent mechanism controlling the barrel cortex excitability (Swadlow, 2002). Furthermore, the blockage of $GABA_A$ receptors caused a widespread astrocytic Ca^{2+} response in previous experiments (Schipke et al. 2008). We therefore wondered whether the increase of neuronal response in our experiments could be due to decreased GABAergic inhibition after astrocytic Ca^{2+} chelation. We studied the effects of bath-applied gabazine ($GABA_A$ receptor blocker) and CGP55845 ($GABA_B$ receptor blocker) on neuronal excitability. Gabazine (Fig.8.a) increased STM depol (N = 9) from 26.3 ± 1.9 mV to 47.5 ± 3.2 mV (186 ± 16%, P = 6 x 10^{-5}). Half rep slightly decreased to 85 ± 17% of control but this was not significant (P = 0.06). ISTM increased from 27 ± 3.8 mV*s to 42.8 ± 6.5 mV*s (162 ± 2%, P = 0.01). During $GABA_A$ receptor blockage we also recorded in seven out of nine neurons APs during the repolarization phase (range: 1 to 7). CGP55845 (Fig.8.b) increased STM depol (N = 10) from 28.4 ± 3.4 mV to 32.5 ± 3.4 mV (117 ± 6%, P = 0.003) and half rep from 0.5 ± 0.05 s to 0.8 ± 0.15 s (154 ± 17%, P = 0.02). ISTM increased from 26.8 ± 7.5 mV*s to 39.8 ± 7.4 mV*s (160 ± 18% P = 0.009). We did not observe APs during the repolarization phase.

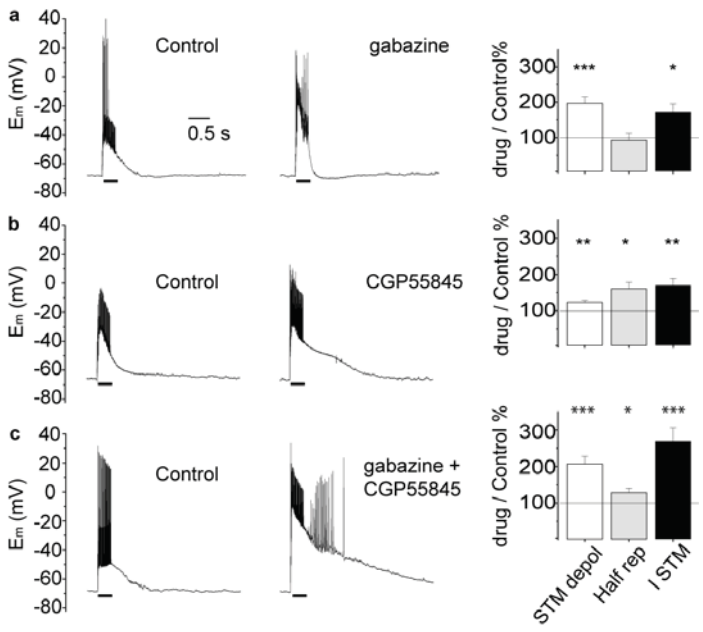

Fig.8 *Inhibiting $GABA_A$ and $GABA_B$ receptors increased the evoked response of barrel cortex neurons.*

a. Membrane potential (E_m) recording of neuronal evoked response in control (left trace) and in the presence of 10 µM gabazine (middle trace). Bar-graph on the right shows the amplitude of stimulus-induced depolarization (STM depol, white column), time for half repolarization (Half rep, gray column) and integral of the voltage trace (ISTM black column). Values refer to evoked response after drug application normalized to the control response (% drug/Control). b, c Effect of 5 µM CGP55845 (b) and combination of 10 µM Gabazine and 5 µM CGP55845 (c). Asterisk; P < 0.05, two asterisks; P < 0.01, three asterisks; P < 0.001 (paired T test between the related parametric values).

Combining $GABA_A$ (gabazine) and $GABA_B$ receptor (CGP55845) antagonists (Fig.8.c, N = 7) increased the STM depol from 23.4 ± 2.6 mV to 46.2 ± 8.4 mV (205 ± 21%, P = 0.0002). Half rep also increased, from 0.5 ± 0.05 s to 0.64 ± 0.1 s (127 ± 12%, P= 0.03), and ISTM increased from 22.8 ± 2.3 mV*s to 60.9 ± 8.3 mV*s (267 ± 36%, P = 0.0006) (Fig.7.c). During the repolarization phase, we recorded APs (9 ± 1.6) from every studied neuron. This data show that both $GABA_A$ and $GABA_B$ activation are necessary to reduce the size of neuronal evoked responses in barrel cortex and to prevent AP firing outside the period of stimulus delivery.

Astrocytic Ca^{2+} chelation, GABA receptor blockage or dialysis with high [Cl^-] reverse a stimulus-induced hyperpolarization into depolarization

To elicit spontaneous AP firing, we depolarized neurons by constant current injection. In such conditions, the barrel stimulation was delivered as described for previous experiments (Fig.9, horizontal bars).

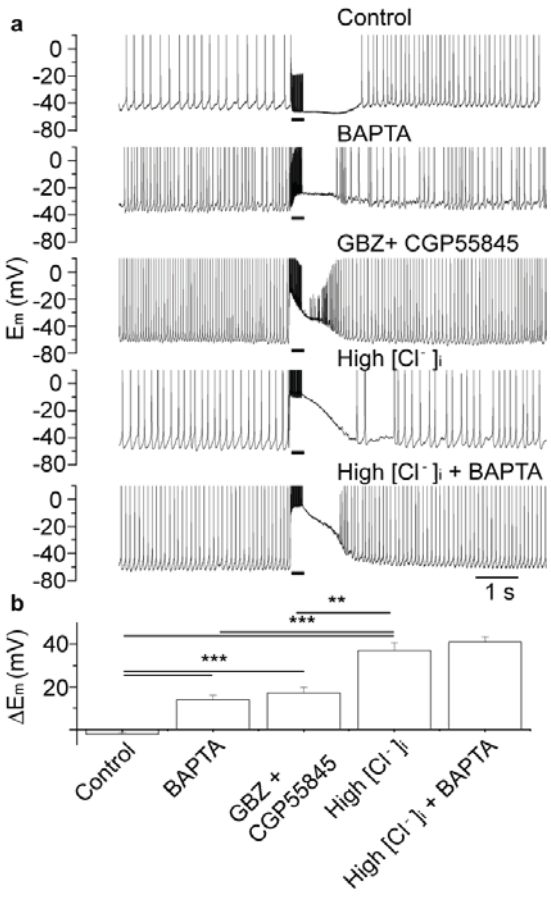

Fig.9 *Astrocytic Ca^{2+} chelation, GABA receptor blockage or neuronal dialysis with high [Cl^-] reverse a stimulus-induced hyperpolarization into depolarization. a. neurons depolarized by tonic current injection constantly fired APs during current clamp recordings of their membrane potential (E_m). Upper three traces: neurons were dialyzed with low [Cl^-] (c.a. 10 mM). Evoked response (stimulation is indicated by bar) before astrocytic dialysis (Control), after astrocytic BAPTA dialysis (BAPTA) and after $GABA_A$ and $GABA_B$ receptor blockage with GBZ (Gabazine) and CGP55845. Evoked response upon neuronal dialysis with high [Cl^-] (132mM) in control (High [Cl^-]) and after astrocytic BAPTA dialysis (high [Cl^-] + BAPTA). (scale bar = 1 s). b. Bar-graph showing average hyperpolarization (Control) and depolarization (BAPTA), (Gabazine +CGP55845), (high [Cl^-]), (High $[Cl^-]_i$ + BAPTA) of evoked responses as described in a. Two asterisks; P < 0.01, three asterisks; P < 0.001 (one-way Anova).*

Upon external stimulation, the APs ceased for about 1 s and the membrane hyperpolarized by -2.2 ± 0.8 mV (N = 13). After astrocytic BAPTA dialysis (N = 10), we observed a depolarization by +14.0 ± 2.0 mV ($P = 5.4 * 10^{-8}$, one-way Anova test; Fig.9). Similarly, in presence of gabazine and CGP55845 (N = 5), the stimulation induced a depolarizing response of +17.6 ± 2.7 mV which was different from control conditions ($P = 1.1 * 10^{-7}$) but not significantly different from the depolarization after BAPTA dialysis (P = 0.3). Astrocyte dialysis with pipette solution without BAPTA led to a transient hyperpolarization by -2.6 ± 1.2 mV (data not shown) as observed in controls (P = 0.8). $GABA_A$ receptors are permeable to chloride ions. Chloride concentration at both sides of the membrane determines whether $GABA_A$ receptors activation is excitatory or inhibitory at a given membrane potential. In our experiments, we can impose the potential across the membrane of the patched neuron (by current injection) as well as the intracellular chloride concentration (whole-cell dialysis). In most of our experimental conditions, $GABA_A$–mediated currents are inhibitory for the patched cell at holding potentials between -65 mV and 0 mV. Consequently, we tested the role of chloride conductance in the neuronal evoked response. For this purpose, we used a high chloride concentration (high $[Cl^-]$) in the patch-pipette (132 mM). We calculated that such conditions would shift the ion's electrochemical gradient in the patched cell and $GABA_A$–mediated responses would be excitatory rather than inhibitory between -65 and 0 mV. After dialysis of a neuron with high $[Cl^-]$ (Fig.9), stimulation triggered a depolarization of +37.0 ± 3.8 mV before astrocytic BAPTA dialysis (High $[Cl^-]_i$) and of +41.0 ± 2.5 mV after astrocytic dialysis (High $[Cl^-]_i$ + BAPTA). These two values were not significantly different from each other (P = 0.4).

Astrocytic Ca^{2+} chelation increases the frequency of APs after stimulation (high $[Cl^-]_i$ in neuron)

In some experiments single neurons were dialyzed with high [Cl^-] through the patch pipette. Cells were then held at c.a. -40 mV by current injection, and, as a result, neurons were constantly firing APs. In these conditions, cells were further depolarized by external stimulation (Fig.9).

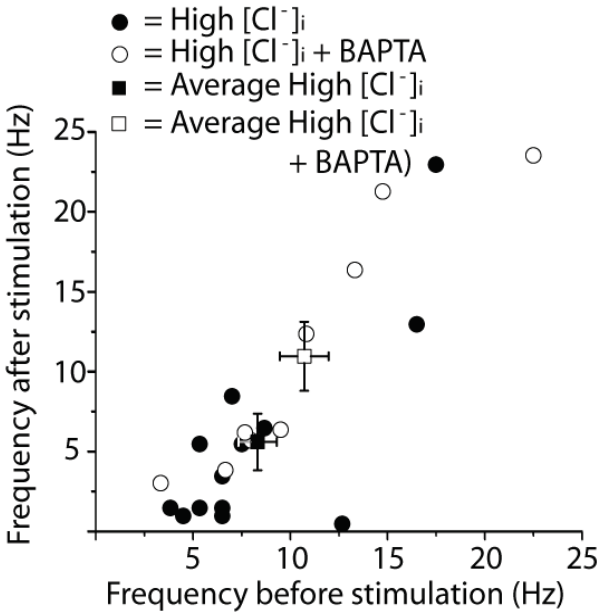

Fig.10 *Astrocytic Ca^{2+} chelation increases the frequency of APs after stimulation. Graph shows AP frequency of neurons dialyzed with high [Cl^-] (as Fig.9, lower traces). AP frequency was determined within two seconds before and after the stimulation. Frequencies after stimulation (vertical axis) were plotted against frequencies before stimulation (horizontal axis). Control (*high [Cl^-] = ●*); after astrocytic BAPTA dialysis (*high [Cl^-] + BAPTA = ○*). Squares represent average values (± SEM) of control (■)and after astrocytic BAPTA dialysis (□).*

After such evoked responses, we observed that the AP frequency was often reduced for a period of about two seconds. This occurred to a lesser extent upon astrocytic BAPTA dialysis (N = 9). To quantify the difference, we measured the AP frequency for two seconds before and after the stimulus delivery in control conditions and after astrocytic BAPTA dialysis (Fig.10). In control conditions (■),

the frequency was reduced to 56%, from 6.7 ± 0.5 Hz before stimulation to 3.4 ± 0.5 Hz after stimulation (N = 27). After astrocytic BAPTA dialysis (□), the firing frequency remained unchanged at 9.6 ± 0.9 Hz and 9.4 ± 1.4 Hz (N = 25).

Neuronal reversal potential shifts from -50 to 0mV upon GABA receptors blockage

Previous experiments (Fig.9) described how a transient hyperpolarization of neurons in control was converted into a depolarization by astrocytic BAPTA dialysis. The same was achieved after blockage of GABAergic receptors or neuronal dialysis with a high concentration of chloride. This and other results suggested the presence of an astrocytic mechanism for neuronal inhibition triggered by external stimulation and dependent on astrocytic intracellular Ca^{2+} elevation. We decided to measure the amount of current underlying such inhibitory mechanism and verify its dependence on astrocytic Ca^{2+}, its nature in terms of ion conductance, and its sensitivity to GABAergic blockers.

We stimulated the neurons in voltage-clamp mode (Fig.11). In these conditions we determined a current / voltage relation of the response in control (“●” N = 8), after astrocytic BAPTA dialysis (“○” N = 8), after Gabazine and CGP55845 application (“▲” N = 8), and after a given neuron was dialyzed with high chloride concentration (“■” High $[Cl^-]_i$ = 132mM, N = 7). For this purpose, we applied a series of voltage steps before and immediately after the stimulation, ranging from -70 to +10 mV (20 mV increment, 30 ms duration).

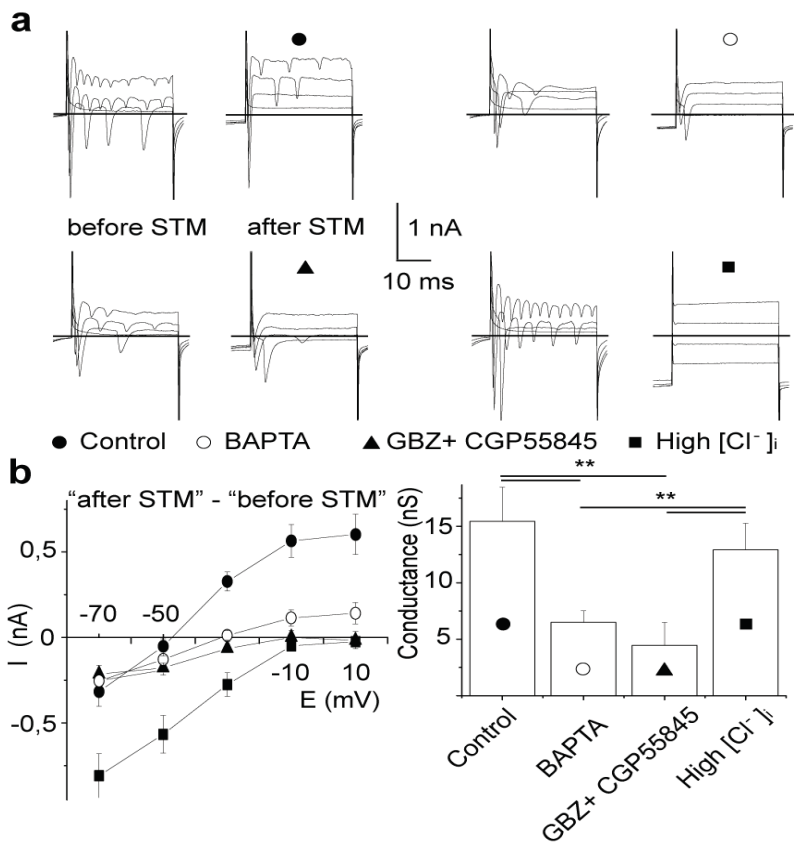

Fig.11 *Reversal potential and membrane conductance are similarly affected by GABA receptors blockage and astrocytic BAPTA dialysis. a. Voltage clamp recordings: currents in response to depolarizing steps (-50 mV, -30 mV, -10 mV and +10 mV) from a holding potential of -70 mV. Recordings were obtained before and after external electric stimulation in control conditions (upper left, ●); after astrocytic BAPTA dialysis (upper right ○); after Gabazine and CGP55845 bath co-application (lower left, ▲); and after neuronal dialysis with 132 mM chloride concentration (high $[Cl^-]_i$) (lower right, ■). (Scale bar: 1 nA, 10 ms) b. Left: Average current / voltage relation of stimulus-evoked conductance under the four conditions described in "a". Right: average conductance between -10 and -70 mV under the four conditions described in "a." (Two asterisks; P = 0.002, One-way Anova).*

In this way, we determined the evoked current before and after stimulus delivery (Fig.11.a). The stimulus-evoked current was then calculated by subtraction (Fig.11.b "after stimulus" - "before stimulus"). The stimulus-evoked conductance (Fig.11.b, right) was also measured from the current / voltage relation (Fig.11.b,

left). The average of the stimulation-induced conductance between -10mV and -50mV was 15.4 ± 3.0 nS in control conditions (●) and the reversal potential was close to -50 mV. After dialysis of astrocytes with BAPTA (○), the conductance was 6.5 ± 1.0 nS, thus significantly decreased in comparison to control (Anova-one-way test, P = 0.002). In this condition, the reversal potential was close to -30 mV. Application of gabazine and CGP55845 (▲) resulted in a conductance of 4.4 ± 2.0 nS with reversal potential of about 0 mV. The stimulus-evoked conductance in presence of Gabazine and CGP55845 was significantly smaller than in controls (P = 0.002) but not different from the conductance after dialysis of astrocytes with BAPTA (P = 0.4). When neurons were dialyzed with 132mM intracellular chloride concentration (■), their average conductance of 12.9 ± 2.3 nS (High $[Cl^-]_i$) was not significantly different from controls (P = 0.4), but the reversal potential was shifted toward positive values (about 0 mV). These results indicate that the barrel stimulation induced an outward current, mediated by GABAergic conductance in neurons. Such conductance is largely based on chloride and depends upon Ca^{2+} elevation in astrocytes as it is largely reduced by astrocytic dialysis with BAPTA. A small inward current was residual to GABAergic blockage. The reversal potential of such current was c.a. 0 mV (see current / voltage relation in Fig.11.b, ▲). We didn't further study such component.

Neurons dialyzed with high $[Cl^-]$ show spontaneous depolarizing events after astrocytes were dialyzed with BAPTA

We decided to determine how astrocytic BAPTA dialysis modulated the neuronal evoked response from resting membrane potential (c.a. – 70 mV) and after neuronal dialysis with high concentration of chloride. Neurons dialyzed through

the patch pipette with 132 mM [Cl^-] (N = 22) showed a large evoked response (Fig.12.a, High [Cl^-]$_i$). The membrane depolarized by 53 ± 2 mV, Half rep was 1.1 ± 0.1 s. and ISTM was 103 ± 9 mV*s. STM depol ($P = 3 * 10^{-10}$), Half rep ($P = 1.5 * 10^{-5}$) and ISTM ($P = 1.6 * 10^{-8}$) were all significantly increased when compared to the evoked response of cells dialyzed with normal [Cl^-] (Fig.12.a, compare to Fig.6.a).

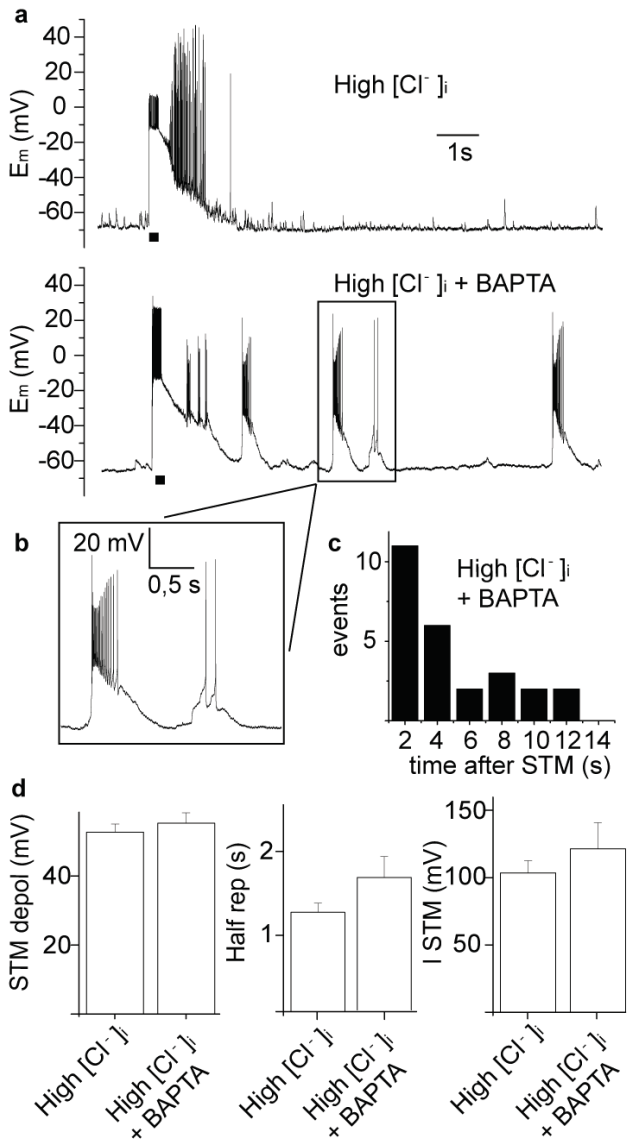

Fig.12 *Neurons dialyzed with high [Cl^-] show spontaneous depolarizing events in the vicinity of BAPTA-dialyzed astrocytes. a. Stimulation (indicated by bar) induced a depolarization in a neuron dialyzed with high chloride concentration before (high [Cl^-]$_i$) and after astrocytic (High [Cl^-]$_i$ + BAPTA) dialysis. b. Spontaneous depolarizing event highlighted in "a" is displayed in higher detail. c. Histogram of spontaneous depolarizations after electrical stimulation. Note that most of the events occurred between two and four seconds after the stimulation. d. Average stimulus-evoked depolarization (STM depol), time for half repolarization ("Half rep") and integral of the voltage trace (ISTM) during the evoked response. Control: "High [Cl^-]$_i$" and after BAPTA dialysis: High [Cl^-]$_i$ + BAPTA.*

This was in line with our previous findings (Fig.9 and 10). Neurons dialyzed with high [Cl^-] typically fired a burst of APs during the repolarization phase.

Surprisingly, in these conditions astrocytic BAPTA dialysis (High $[Cl^-]_i$ + BAPTA, N = 15) did not affect the parameters of the evoked response (Fig.12.d). After astrocytic dialysis STM depol was 55 ± 3 mV (P = 0.5), Half rep was 1.7 ± 0.3 s (P = 0.14) and ISTM was 120 ± 19 mV*s (P = 0.4). After astrocytes were dialyzed with BAPTA, we observed, however, a new behavior in some neurons (eight out of 15). Spontaneous depolarizing events (Fig.12.a and b) occurred after the initial, stimulus-related depolarization. The highest incidence of such events was between two and four seconds after the stimulation (Fig.12.c).

The average amplitude of the spontaneous depolarizing events was 22 ± 3 mV; their Half-rep was 0.9 ± 0.5 s. During such depolarizations (Fig.12.b) neurons fired on average 9 ± 3 APs. Such events were not observed in control or in any other experimental conditions.

$GABA_B$-mediated neuronal inhibition

Since $GABA_B$ receptor blockade prolonged the Half rep (Fig.8), we measured the effects of $GABA_B$ pharmacological stimulation on the neuronal response. For this purpose, neurons were dialyzed either with low (N = 6) or high intracellular chloride concentration (N = 7) (Fig.13.a and b).

In such conditions, the barrel was stimulated after 15 to 60 minutes of baclofen incubation. Evoked responses of different cells stimulated in the absence of baclofen are reported as control.

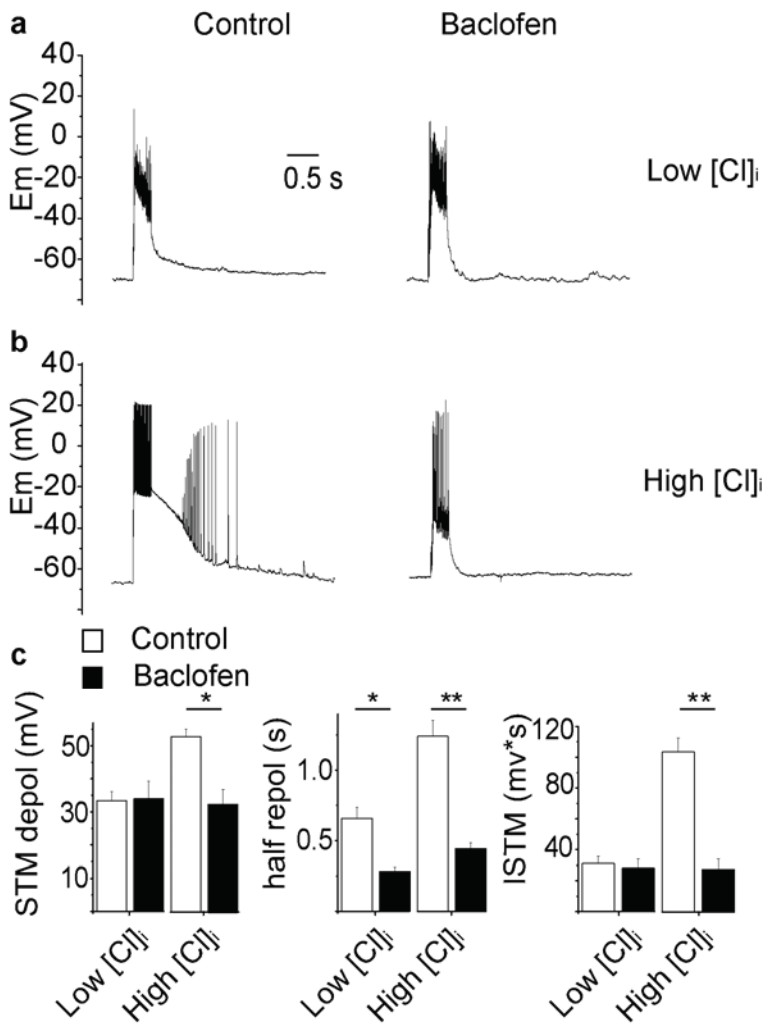

Fig.13 *Stimulating $GABA_B$ receptors with 20 μM baclofen decreased the stimulus-induced depolarization. Cells were dialyzed with low (a) and high [Cl^-] (b). Neuronal evoked responses (E_m) in control (left) and in the presence of baclofen (right). c. Bar-graphs of the average stimulus-evoked depolarization (STM depol), half repolarization (Half rep) and integral of evoked response (ISTM) from controls (white columns) and upon baclofen application (black columns). Each graph shows couples of values for "Low $[Cl]_I$" and "High $[Cl]_I$" One asterisk; P < 0.05, two asterisks; P < 0.001, (unpaired T test).*

When neurons were dialyzed with low intracellular [Cl^-], baclofen caused a limited decrease of the evoked response (Fig.13.a). Half rep was decreased (P < 0.01) to 0.36 ± 0.06 s (Fig.13.c) but significant changes didn't occur in the STM-evoked depolarization or in ISTM (P > 0.5). In contrast, when neurons were dialyzed with high [Cl^-], baclofen greatly suppressed their evoked response (Fig.13.b). STM depol during baclofen perfusion was now 33 ± 1 mV (Fig.13.c). Half-rep was 0.44 ± 0.04 s and ISTM was 27 ± 6 mV*s. These values were significantly smaller in

comparison to controls (One asterisk: P < 0.01, two asterisks: P < 0.001, unpaired T-Test). Some APs were visible in presence of baclofen as in controls when neurons were dialyzed with high [Cl^-]. The size of evoked response after high [Cl^-] neuronal dialysis and after baclofen application was not otherwise different from the response evoked with low intracellular [Cl^-] in control conditions.

Ionotropic glutamate receptor blockers have only a marginal effect on the neuronal evoked response

Glutamate is the principal excitatory neurotransmitter in the cortex. In our experiments, the stimulation electrode was placed directly in the cortex (L4), in close proximity to the cellular processes of virtually every neuron we patched. Part of the evoked neuronal depolarization could be therefore directly elicited by the electrical stimulator rather than by glutamate-mediated neurotransmission. To quantify the proportion between these two components of the neuronal evoked excitation, we blocked AMPA-kainate receptors with CNQX (Fig.14.a).

In such conditions, we found no significant differences in STM depol (P = 0.07), Half rep (P = 0.2) and ISTM (P = 0.1) in comparison control (N = 7). NMDA receptor blockage with MK801 (Fig.14.b) significantly decreased the Half rep from 0.64 ± 0.1s to 0.51 ± 0.04 s (85 ± 6% of internal control) but did not affect STM depol (P = 0.1) nor ISTM (P = 0.07), (N = 8). Joint blockage of both AMPA-kainate and NMDA receptors (Fig.14.c) did not affect STM depol (P = 0.06) but decreased Half rep from 0.87 ± 0.13 s to 0.7 ± 0.06 s (83 ± 6) and ISTM from 25.9 ± 6.7 mV*s to 17.4 ± 3.6 mV*s (88 ± 6%),(N = 5).

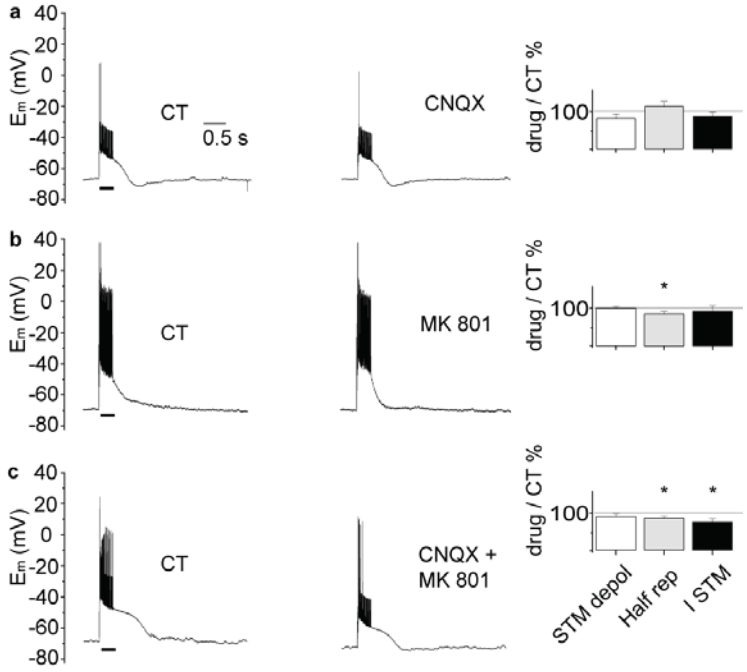

Fig.14 *Ionotropic glutamate receptor blockers have only marginal effect on the neuronal evoked response. Membrane potential (E_m) during stimulation (indicated by bar): before (CT) and during application of 20μM CNQX (a), 10μM MK801 (b) and combined application of CNQX and MK801 (c). On the right: average amplitude of stimulus–evoked depolarization (STM depol, white) half repolarization time (Half rep, gray) and integral of the evoked response (ISTM, black) normalized to control. Asterisk; P = 0.03 (paired t- test of the related parametric values).*

We therefore observed that the glutamatergic synaptic transmission contributes only moderately to overall neuronal excitation during the stimulus-evoked response. We conclude that in our experiments neurons were mostly directly depolarized by electrical stimulation. How gap-junctions between neurons can affect the spreading of depolarization between neighboring cells remains to be quantified.

Metabotropic Glutamate receptors, purine receptors, and D-serine modulation play only a minor role in the control of the evoked neuronal response

We tested the impact of mGluRs stimulation and blockage on neuronal activity. This could have been a relevant mechanism since mGluRs have been described as involved in neuron-glia communication (Newman et al. 2003, Wang et al. 2006). The mGluR1, 2 and 5 agonist "*trans*-ACPD" (100 μM) evoked a sustained astrocytic Ca^{2+} elevation (ΔF/F = 11.2 ± 2%, not shown). The effect lasted for the whole duration of agonist perfusion (60 s) and was reversible upon washout. During drug application, the local electric stimulation caused no further Ca^{2+} increase in astrocytes, but the usual barrel Ca^{2+} response was restored after washout. In the presence of *trans*-ACPD, the stimulus-evoked response in neurons was not significantly affected ($0.09 < P < 0.1$). In these conditions, three of 13 cells fired 24 ± 4 APs during the repolarization phase. The application of the mGluR1 and mGluR5 antagonists LY367385 and MPEP (N = 8) did not affect the area of astrocytic response (149 ± 22%, n = 8%, P = 0.08). In such conditions, the neuronal evoked response was only marginally changed, namely the block of mGluR1 and mGluR 5 caused an increase in Half rep from 0.56 ± 0.1s to 0.63 ± 0.1s (P = 0.02).

Glycine may play a role in the brain as an inhibitory neurotransmitter (Zeilhofer et al., 2005). We therefore examined whether glycine blockage would affect the neuronal evoked response. To achieve this, we applied strychnine, a glycine receptor blocker (N = 5). In such conditions, we observed a modest suppression of the neuronal evoked response: Half-rep was shortened from 0.52 ± 0.09 s to

0.37 ± 0.05 (P = 0.04). We did not measure the astrocytic evoked response during strychnine application.

Adenosine inhibits the neuronal activity and is an important gliotransmitter in other parts of the central nervous system (Serrano et al. 2006), (Halassa et al., 2009). We therefore tested the possible effects of an adenosine (A_1) receptor blocker (CPT) in the barrel cortex. CPT at the concentrations of 4 µM (Tab.1, N = 12) or 20µM (N= 5, data not shown) did not significantly affect any parameter of the neuronal evoked responses (0.5 < P < 0.8). This drug also failed to affect the astrocytic evoked responses. Upon CPT application (CPT), the average size of the astrocytic response was the same as before drug application (CT) (CPT / CT = 114 ± 16% P = 0.4).

D-serine is a modulator of ionotropic glutamatergic receptors. This amino acid is released by the astrocytes upon Ca^{2+} elevation and was shown to be essential for neuronal plasticity in hippocampus (Hennenberger et al. 2010). In our system, in contrast, the slice incubation of the brain slice with D-serine-synthetase inhibitor D-AAO (Tab.1, N = 4) failed to induce any detectable difference in the evoked neuronal response. For these experiments, we used other untreated neurons as control (Fig.3), None of the evoked-response parameters in presence of D-AAO was found significantly changed from controls (P > 0.05, Unpaired T-test).

To summarize these results: the signaling pathways involving glutamate, purines, glycine, and D-Serine do not play a dominant role in the astrocytic modulation of neuronal evoked response in the context of our study in barrel cortex. The effects of *trans-ACPD* suggest that mGluRs could be marginally involved in inhibiting the neuronal evoked response. LY367385 and MPEP, however, didn't affect the astrocytic or neuronal evoked response in the opposite direction.

	STM depol. (mV)		**Half rep.** (ms)		**I STM** (mV*s)		**neurons firing during repolarization**
	Control	drug	Control	drug	Control	drug	drug
trans-ACPD	25.1 ± 0.6	26.9 ± 2.7	0.73 ± 0.10	1.09 ± 0.28	29.0 ± 3.8	45.3 ± 11.8	3 out of 13
LY367385+MPEP	32.1 ± 3.2	36.4 ± 3.5	0.56 ± 0.13	0.63 ± 0.14 *	24.8 ± 1.8	25.4 ± 2.4	1 out of 8
CPT	23.7 ± 1.8	22.6 ± 1.5	0.65 ± 0.12	0.68 ± 0.08	20.5 ± 2.5	19.5 ± 2.0	1 out of 12
Strychnin	33.1 ± 1.9	34.0 ± 2.2	0.52 ± 0.09	0.37 ± 0.05 *	25.7 ± 4.0	21.4 ± 2.7	0 out of 5
D-AAO		29.2 ± 3.5		0.47 0.01		24.6 ± 7.1	0 out of 4

Tab.1 *mGluR, glycine, purinergic receptors and serine release did not affect the neuronal evoked depolarization. In each row, the average stimulus-evoked depolarization (STM depol), half repolarization (Half rep.) and integral of stimulus-evoked response (ISTM). Paired values are reported before (Control) and during drug application (drug). Asterisk; P < 0.05 (paired T-test). The column on the far right gives the number of cells in which APs were recorded during the decay phase of evoked response upon drug application. Drug concentrations: trans-*ACPD, *200 µM LY367385, 100 µM MPEP, 4 µM CPT, 5 µM strychnine, 17U/ml D-AAO.*

Spontaneous activity of barrel cortex neurons

Our paradigm of progressive astrocytic dialysis with BAPTA requires approximately one hour (45 to 60 minutes). After such dialysis, the neuronal evoked response was increased (see previous results). We reasoned that the GABAergic inhibition of neuronal evoked responses could be part of a tonic mechanism of gliotransmitter release rather than a transient consequence of astrocytic Ca^{2+} fluctuation. Given the long time required for the dialysis, we found it conceivable that our paradigm could condition the neuronal network throughout the entire period (45-60 minutes) necessary for BAPTA to spread. If so we could expect the neuronal excitability to be increased upon BAPTA dialysis even when the barrel stimulation is not applied. To verify this, we measured the synaptic activity of barrel neurons omitting our paradigm of local network stimulation.

Excitatory post-synaptic currents (ePSCs) were measured during baseline recordings from L4 and L2/3 neurons (Fig. 15.a). In these conditions, we observed that astrocytic BAPTA dialysis increased the frequency of spontaneous ePSCs, (Fig. 15.b): from 0.3 ± 0.03 Hz in control conditions (n = 11) to 0.8 ± 0.2 Hz after BAPTA dialysis (N = 8, P = 0.01). No other changes were observed: ePSCs amplitude (16 ±2 pA, control and 13 ± 1 pA, BAPTA) and ePSC decay constant (4.7 ± 2 ms, control and 7.7 ± 1 ms, BAPTA) were unchanged (P = 0.1, P = 0.1). The average neuronal access resistance (R_a) was 22 ± 0.9 MΩ (17 MΩ < R_a < 30 MΩ) in control and 21.6 ± 0.6 MΩ (20 MΩ < R_a < 25 MΩ) after astrocytic dialysis (P = 0.6).

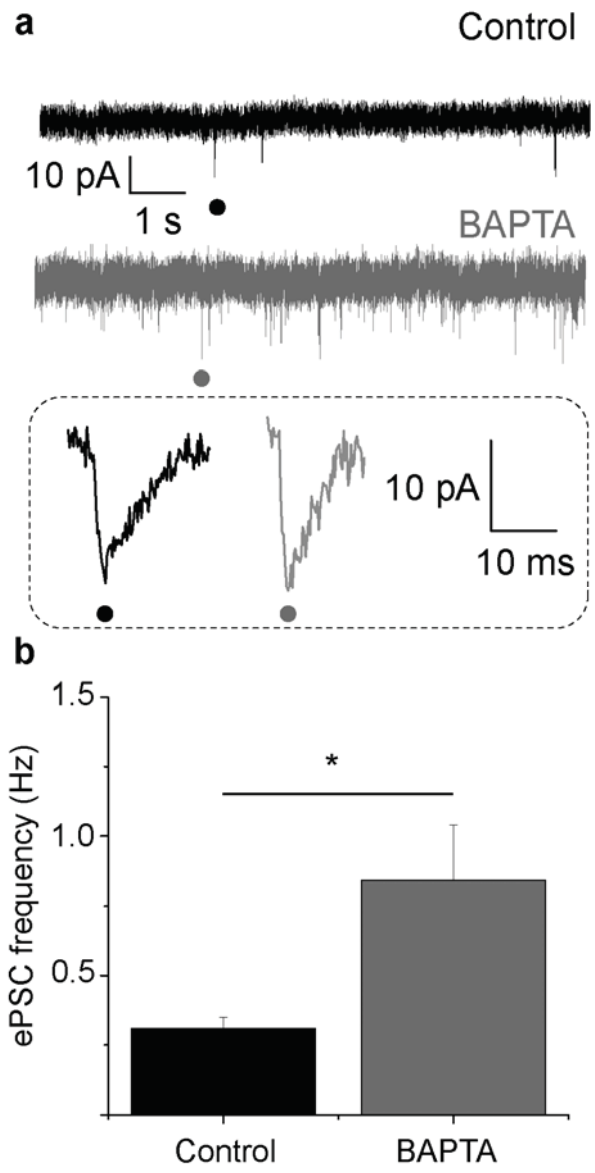

Fig.15 *Astrocytic Ca^{2+} chelation increased the frequency of spontaneous excitatory post synaptic currents (ePSC). a. representative sample of voltage clamp recording. Holding potential is -70mV in control (black) and after astrocytic Ca^{2+} chelation (gray). Single events (●) are displayed at higher magnification in the frame below. b. ePSC frequency is significantly increased after astrocytic Ca^{2+} chelation (one asterisk: P = 0.01).*

The resting membrane potential (E_m) was also not significantly different (P = 0.4) between neurons in control (E_m = -67.9 ± 1.5 mV) and after astrocytic dialysis (E_m = -68.5 ± 0.8 mV). Moreover, we did not observe any seizure-like event or other types of spontaneous membrane potential oscillations in control conditions after astrocytic dialysis with BAPTA.

Stimulus delivery and ePSC frequency

We monitored the ePSC frequency before and after local barrel stimulation (Fig. 16.a).

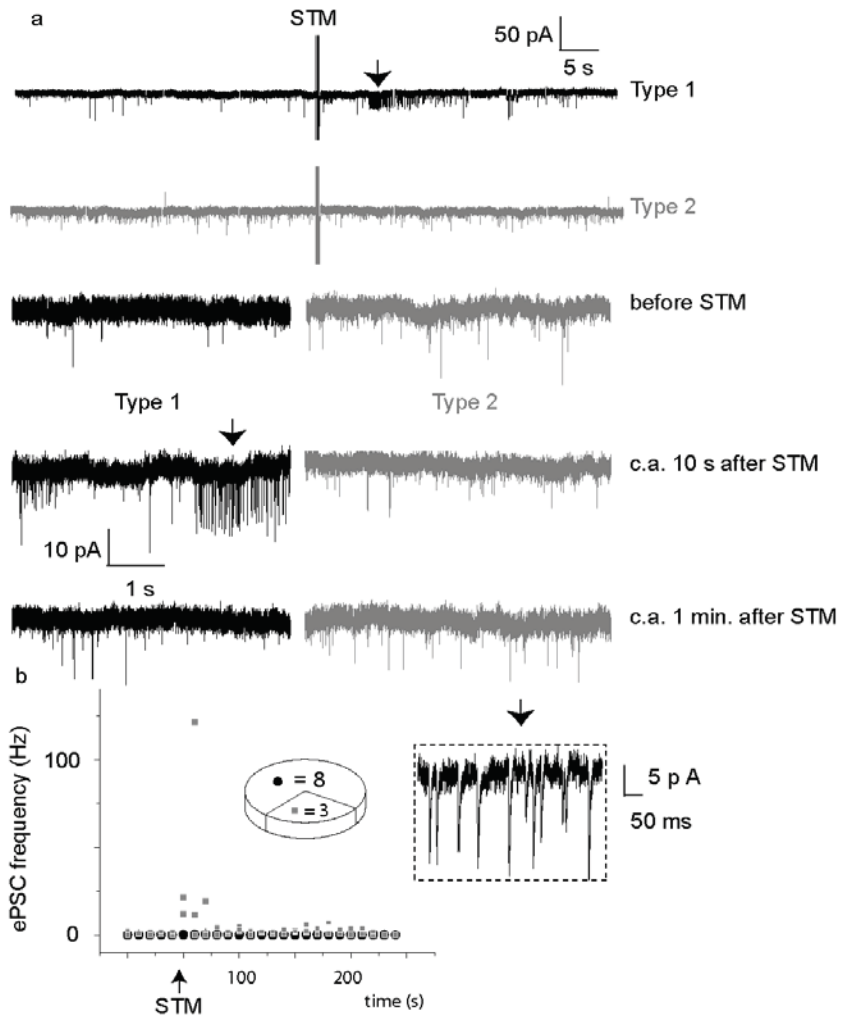

Fig.16 *Effects of local stimulation on ePSC in barrel neurons. a. Two samples of baseline activity before and after stimulation (STM) marked by vertical bar. Below, the same traces before stimulation (STM), c.a. 10 s and c.a. 1 minute after STM. Note in "Type 1" (black): ePSC frequency transiently increased after STM (marked by vertical arrow), in "Type 2" (gray) ePSC frequency was unchanged. b. Graph shows the time course of ePSC frequency (average on 10 s baseline blocks) for Type 1 (■ = 3) and Type 2 (● = 8) neurons. On the right side in dashed square: sample of ePSCs during the frequency increase at higher resolution (marked by arrow as in a).*

We observed in some cells (Type 1) a transient increase in ePSC frequency c.a. 10 s to 30 s after stimulus delivery (n = 3). After this period the ePSC frequency recovered to control values (Fig.16.b). In most neurons (Type 2), no change in the

ePSP frequency was observed (N = 8). Astrocytic BAPTA dialysis (N = 5) did not have any detectable consequences on neuronal ePSCs frequency after stimulation: 102 ± 2% in controls (P = 0.3) and 112 ± 34% after astrocytic dialysis (P = 0.7).

Short- and long- term effects of astrocytic Ca^{2+} chelation

We wondered whether the glial GABA transporter (GAT 2/3) might play a role in our system. GAT 2/3 could, for instance, work in a reverse manner in a Ca^{2+}-dependent fashion. Alternatively GAT 2/3 could increase GABA concentration inside astrocytes that would then release it through some other mechanism. Thus, we pharmacologically blocked GAT 2/3 to alter GABA “ambient” concentration (Kirmse, Kirischuk & Grantyn, 2009). For this purpose, we tested the effects of the specific blocker, SNAP5114, on the neuronal evoked response. We studied whether the block of glial GABA transporters would mimic the effects of astrocytic BAPTA dialysis. We incubated brain slices with SNAP 5114 for different periods and found that the blockage of GAT 2/3 affects the neuronal evoked response after a long but not after a short incubation (Fig.17, a, b, d).

Namely, with a long SNAP5114incubation (15 to 60 minutes) the neuronal evoked response was significantly prolonged (Fig.17.a): Half rep was 1.84 ± 0.18 s (P < 0.001) and ISTM was 203 ± 17 mV*s (P < 0.001) (Fig.17.b). Such effects were significant either comparing the neuronal evoked response to unpaired or paired controls (Fig.3). STM depol, by contrast, was unchanged in comparison to control conditions and equal to 23.3 ± 2.6 mV (P = 0.1).

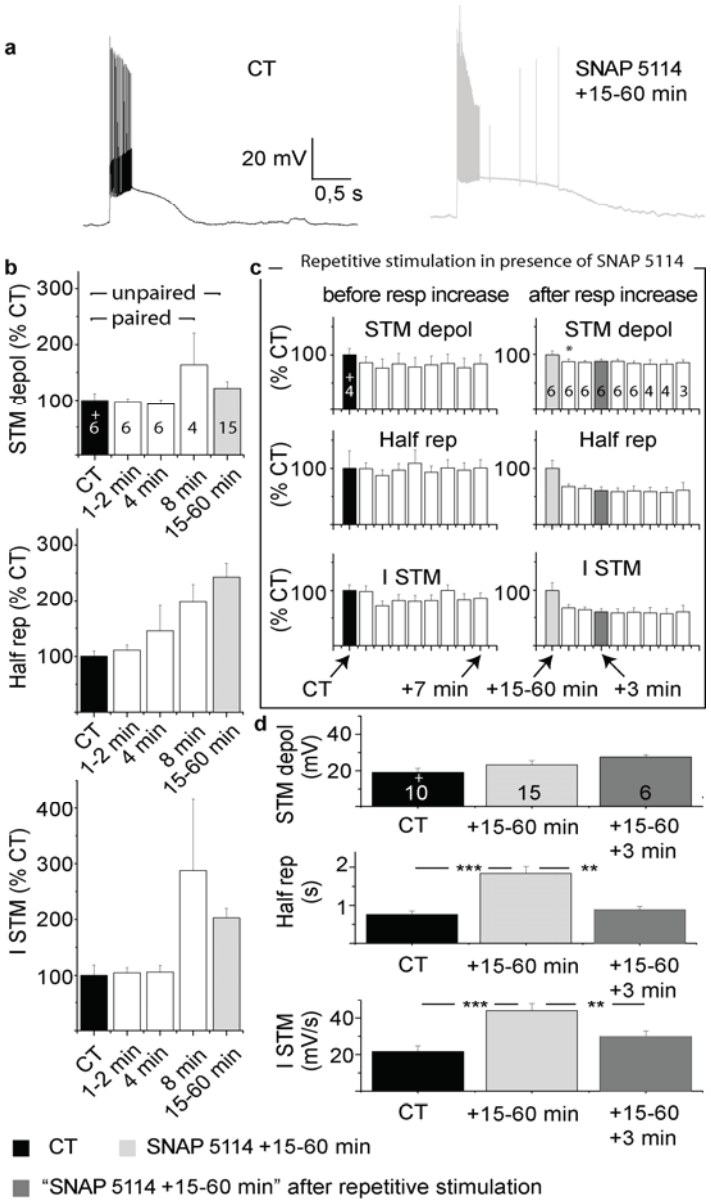

Fig.17 *SNAP 5114 increases neuronal evoked responses after more than 15 minutes of drug perfusion. a. sample of neuronal evoked response in control (black) and after prolonged incubation with (15 to 60 minutes) SNAP 5114 . b. time progression of respectively evoked depolarization (STM depol), half repolarization (Half rep) and integral of the evoked response (ISTM) in control (black) long-term drug application (gray) and intermediate time points (white). Responses in the presence of SNAP5114 are normalized to control (% CT). c. as in "b": time course of the evoked-response upon frequent (every 60 s) stimulation. Left side: frequent stimulation (before resp. increase) starting from control conditions (black). Right side: frequent stimulation (after resp. increase) starts after SNAP5114 application (light gray). D. control evoked response (black) average response after SNAP5114 application (light gray) and response adaptation due to frequent stimulation (dark gray).*

The effects of SNAP 5114 were not prominent after shorter periods of incubation: two or four minutes (N = 6) had no significant effects on the neuronal evoked

response (Fig.17.b, white columns $0.1 < P < 0.5$). Mild effects were visible after eight minutes (Fig.17 right white column, N = 4): Half-rep was increased to 1.69 ± 0.19 s ($P = 0.01$), STM depol was 22.0 ± 4.3 mV and ISTM 47.1 ± 11.5 mV*s. The two latter values were not significantly different from controls (respectively $P = 0.07$ and $P = 0.1$).

After a long SNAP5114 incubation (15-60 min), we stimulated the barrel cortex at high frequency (interstimulation interval of c.a. one minute) and observed a progressive depression of the evoked response (Fig.17.c). Upon frequent stimulation the evoked response was decreased from the second stimulus repetition: STM depol was 87 ± 5% of control, Half rep 66 ± 4% of control, ISTM 67 ± 6% of control (N = 6). The response was then stable upon further stimulus repetitions (Fig.17 dark gray bars). If the stimulus repetition was applied immediately after SNAP5114 perfusion (N = 4), no significant changes in the evoked response were instead observed ($0.1 < P < 0.3$).

As SNAP 5114, other neuromodulators (including substances that failed in the short-term application) might affect the barrel evoked response only after a long period of incubation. This needs to be assessed in future experiments.

DISCUSSION

In the present work, we investigated the neuronal and astrocytic activity in the juvenile mouse barrel cortex. We studied a type of neuronal activity that induces a local and transient Ca^{2+} increase in neighboring astrocytes. We found in this context that the astrocytic Ca^{2+} response mediates neuronal inhibition. Our data indicate that GABA is primarily involved in this inhibitory interaction between astrocytes and neurons. In the following chapter, these results and their possible implications are discussed in detail.

Electrophysiological recordings in barrel cortex were obtained from excitatory neurons

The samples we chose in our study belonged to a heterogeneous group of excitatory neurons: pyramidal cells, spiny stellate cells, and star-pyramidal cells (Fig.1). Interneurons, which make up the minority (ca. 10%) of all neurons in the cortex (Lefort et al., 2009), were a difficult target and were excluded from our selection. As sampling criteria, we chose the shape of cell somata: triangular for pyramidal cells (L2/3) and small and round for spiny stellate cells (L4). We avoided selecting elongated-elliptical somata or neurons in L2/3 that appeared devoid of apical dendrites. The targeted cells were also characterized by recording their AP firing patterns during patch clamp experiments. Neurons were typically “regular spiking” (Fig.1). Such firing pattern was commonly associated with pyramidal neurons (Chagnac-Amitai & Connors, 1989), spiny stellate neurons and star-pyramidal neurons (Feldmeyer et al., 2005). In contrast, a “fast spiking” pattern was commonly associated with interneurons (Bacci et al., 2002),

(Beierlein et al., 2003), (Sun et al., 2009) but was not usually encountered in our sampling. When this did occur, we would not use the cell for further investigation. We are aware that some interneurons display other patterns of APs rather than “fast spiking” (Markram et al., 2004). Some of these resemble the “regular spiking” type. For this reason, some interneurons could have been included by chance in our sampling. If this was the case, it was only a small fraction of all analyzed samples. To get a clearer picture about the cells investigated, the detailed morphology of some samples was reconstructed at the confocal microscope after tissue fixation and staining (Fig.1). The morphology of the reconstructed neurons corresponded to previous descriptions of pyramidal cells and spiny stellate cells (White & Rock, 1980), (Lubke et al., 2000), (Feldmeyer et al., 2002), (Lubke et al., 2003), (Lubke & Feldmeyer, 2007), (Fox, 2008). Most of the neurons we observed were endowed with dendritic star-like branching and long longitudinal axonal projections occasionally reaching the white matter. Cell somata were usually triangular or round with occasional apical dendrites toward L2/3 as described for star-pyramidal neurons. In some of these cells, we also observed the anisotropic distribution of dendrites as described for spiny stellate cells (Feldmeyer et al., 1999). Interneurons are described in their various shapes (Fox, 2008), (Markram et al., 2004). A common feature for some of them is the smaller extension of their processes compared to excitatory neurons (Lubke et al., 2000),(Lubke et al., 2003), (Fox, 2008). As two of our samples lacked long axonal projections, we could not be entirely sure about their classification as excitatory cells. Their AP pattern, however, was “regular spiking.” On the base of our classification criteria, we found that 19 out of 21 regular spiking neurons were morphologically recognizable as excitatory cells. We conclude that referring to

these cells as excitatory neurons is a fairly correct approximation and that the AP firing pattern is a reliable predictor for the identity of the targeted cell.

Dye-coupling between L4 and L2/3 neurons

During the process of morphological analysis, we dialyzed single cells through the patch pipette solution which contained biocytin. This small molecule is highly diffusible but membrane-impermeable. We found, after fixation and labelling, that biocytin had spread to neurons neighboring the one we patched (Fig.1). This happened in about half of our experiments (Fig.2) and implied that those cells were coupled through gap-junctions. Occasionally, we observed also that not just the neighbouring neurons were coupled but so were some distant cells (in other barrels) touched by collateral projections of the neurons we patched. Developmental coupling between pyramidal neurons has been previously reported (Priest et al., 2001). According to the literature, neurons can be electrically coupled only with other neurons of the same kind and coupling is only lasting during developmental stages. Coupling between L4 granular neurons was instead not reported so far. Although this matter is secondary to the purpose of our research, it is interesting in light of the finding that blockage of AMPA and NMDA receptors had only a limited effect in suppressing the neuronal evoked response (Fig. 14). It is tempting to speculate that the spreading of second messengers or electrical coupling (Rorig & Sutor, 1996) might play a role in synchronizing the depolarization observed in our experiments (Fig.3). But this needs to be tested in future experiments. We also remarked that local electrical stimulation (in L4) was likely to account in large part because of the synchrony in the neuronal evoked response.

Characterization of the neuronal evoked response in the barrel cortex

We adopted a paradigm of barrel electric stimulation that was shown to reliably elicit astrocytic Ca^{2+} responses (Schipke et al., 2008). So far, the neuronal activity evoked by such stimulation has not been described. Here we found that virtually all neurons in the stimulated barrel incurred a synchronous depolarization (Fig.3). Such a slow depolarization event was coincident with a burst of APs during the period of stimulus delivery (300 ms). This type of neuronal activity closely resembles a paroxysmal depolarization shift as reported in the literature upon synaptic impairment and epileptic induction (Mutani, 1986), (Gutnick, Connors & Prince, 1982), (Konnerth, Heinemann & Yaari, 1986), (Deisz, Billard & Zieglgansberger, 1997), (Chagnac-Amitai & Connors, 1989), (Sutor & Luhmann, 1998), (Marescaux et al., 1992), (Vergnes et al., 1997), (Harris & Stewart, 2001), (Konnerth et al., 1986). In some respects, however, the response we evoked was remarkably different from a paroxysmal epileptic shift. In most of the mentioned bibliography, a long-lasting conditioning paradigm was applied to induce such a type of neuronal activity. Thus, epilepsy and spontaneous seizures occur in a network that has undergone a pathological transformation. Our stimulation, in contrast, led to a single event at the end of which the membrane potential recovered to resting voltage. After stimulation, we did not observe long-lasting differences in the intrinsic electric membrane properties or ePSC frequency (Fig.16). Furthermore, epileptic models based on electric kindling typically require numerous (tens to hundreds) stimulus repetitions (Goddard, McIntyre & Leech, 1969), (Sutula, Cavazos & Woodard, 1994), (Powell et al., 2008). In contrast, in our experiments the stimulus repetition was mostly limited to two evoked and

timely distant events. If the stimulus was applied repeatedly at intervals of about two minutes or about 60 minutes the evoked response was unchanged (data not shown). This implies that our study should not be regarded as referring to a pathological status of the brain. Yet, the evoked response we triggered was prominent and likely to exceed the usual neuronal activity of the brain *in vivo*.

The neuronal evoked response was prevented by TTX. Thus, it required the opening of voltage-gated sodium channels. Probably Ca^{2+} channels contributed as well to the depolarization of the barrel neurons given that neuronal Ca^{2+} transients were described in previous works (Schipke et al., 2008). Ca^{2+} currents were not characterized in detail in the course of our experiments. As mentioned above, AMPA and NMDA receptors played a minor role in the evoked neuronal depolarization (Fig.14). GABAergic receptors were largely involved in inhibiting the evoked response. $GABA_A$ receptors limited the amount of depolarization during the period of stimulus delivery. $GABA_B$ receptors shortened the time for a complete repolarization to resting membrane potential. Our results are therefore in agreement with previous reports about a prominent GABAergic inhibition in barrel cortex (Swadlow, 2002), (Teichgraber et al., 2009). Probably interneurons are accountable for such a mechanism to a large extent (Swadlow, 2002). It is however possible that astrocytes contributed to such GABA-mediated inhibition (Kozlov et al. 2006), (Lee et al., 2010).

The average neuronal depolarization outside the stimulated barrel was smaller than within the stimulated barrel. Several neurons were synchronously firing APs. Such activity was not sufficient to evoke astrocytic responses. This finding is in line with what has been observed *in vivo* (Wang et al., 2006), namely, the authors

reported that not all the stimuli delivered to the whiskers could evoke astrocytic Ca^{2+} responses in the cortex. In essence, several frequencies of stimulation failed to recruit astrocytic responses although the recording of local field potentials clearly showed the presence of stimulus-associated neuronal activity. We propose that the large synchronous neuronal depolarization and AP firing is a necessary condition to evoke a widespread and synchronous astrocytic Ca^{2+} response. These are also the probable experimental conditions of several other publications (Wang et al., 2006), (Serrano et al., 2006), (Andersson & Hanse, 2010). This would furthermore be consistent with the finding that, upon $GABA_AR$ pharmacological blockage, a larger spreading of astrocytic-evoked responses was observed (Schipke et al. 2008), probably due to a larger neuronal recruitment across neighboring columns.

Ca^{2+} chelation in astrocytes

To block the astrocytic Ca^{2+} response, we selectively dialyzed these cells with BAPTA (40 mM). The efficiency of this procedure has been shown in previous publications (Serrano et al., 2006) (Andersson & Hanse, 2010). Since some authors reported problems in the optimization of such a paradigm (Serrano et al. personal communication), we decided to assess independently the procedure efficiency with dye-coupling experiments (sulforhodamine B) and with Ca^{2+}-imaging experiments. In our hands, dye-coupling revealed networks of six to 12 coupled cells up to ~200 µm from the patched astrocyte. The procedure was not harmful to neurons or astrocytes since after dialysis their resting potential and access resistance were unaltered. Astrocytic Ca^{2+} chelation, nevertheless, increased the spontaneous ePSC frequency in neurons. Given the astrocytic

capability of releasing glutamate (Parpura et al. 1994), (Kang et al., 1998), GABA (Angulo et al., 2008), (Lee et al., 2010) or ATP (Serrano et al., 2006) such modulation of ePSC frequency could have been caused by the impairment of several Ca^{2+}-dependent gliotransmission pathways. A possible explanation of the increased ePSC frequency upon astrocytic dialysis could be the impairment of tonic release of either of these molecules. We did not further characterize gliomodulation of ePSC as our research was mainly focused on evoked synchronous responses.

Astrocytes mediate neuronal inhibition

Several experiments in our research line showed independently that the neuronal excitability was increased upon astrocytic Ca^{2+} chelation. We also noticed some remarkable similarities between the effects of such astrocytic manipulation and those of GABAR pharmacological blockage. Furthermore, in several experiments we observed that other potential gliotransmitters failed to modulate the neuronal evoked response. Regrettably, we did not find a molecular pathway which can pinpoint the gliotransmission and Ca^{2+}-dependent neuromodulation that we describe. What we observed could be caused by a direct inhibitory mechanism, such as the astrocytic release of GABA, or an indirect mechanism, such as, the potentiation of interneurons induced by Ca^{2+}-mediated release of another gliotransmitter. Mindful of this uncertainty, we will summarize the achieved results and discuss their implications.

Astrocytic Ca^{2+} increase is inhibitory to neurons in the juvenile mouse barrel cortex:

1. In control conditions, the astrocytic Ca^{2+} response was restricted to a single barrel field (Fig.3). The local dialysis with BAPTA caused a decrease in their response within the stimulated barrel. At the same time, the evoked astrocytic response was widespread over several barrel fields (Fig.5). This result had a striking resemblance to what was achieved previously (Schipke et al., 2008) upon $GABA_A$ receptor blockage. Originally, this set of experiments was only planned as a quality assessment of the dialysis efficiency. However, the result achieved only confirmed the appropriateness of our methodology. As with previous publications (Schipke et al., 2008), it suggested that astrocytic Ca^{2+} chelation has similar consequences for the barrel cortex as the block of GABA receptors (i.e. an increase of neuronal excitability). By the time those experiments were performed, we mainly expected adenosine to be the potential gliotransmitter candidate for the barrel inhibition (Serrano et al., 2006) or, as an alternative, the occurrence of glutamate-mediated interneuron potentiation (Kang et al. 1998, Liu et al. 2004). Further experiments (discussed later) showed that these mechanisms are instead unlikely to apply to our system. At this stage, we wondered if the mere stimulus repetition (rather than astrocytic dialysis) might trigger an enlargement of astrocytic response. As a result, we applied the control stimulation at intervals of c.a. 60 minutes. We observed that, in absence of further manipulations, the mere stimulus repetition left the evoked Ca^{2+} response unaltered.
2. When astrocytic Ca^{2+} was chelated the evoked neuronal response was increased (Fig.6). To be sure that we genuinely impaired a form of Ca^{2+} -

mediated gliotransmission, we similarly dialyzed astrocytes with a solution containing potassium-gluconate instead of BAPTA (Fig.7). This had no consequences for the neuronal evoked response. We therefore concluded that the blockage of Ca^{2+} in astrocytes impaired a mechanism of gliotransmission responsible for the barrel network inhibition. In light of this finding, we noticed that *in vivo* the local field potential seems suppressed by astrocytic Ca^{2+} elevation (Wang et al., 2006). Regrettably, the authors did not comment on or statistically consider such phenomenon. The larger neuronal evoked response together with the previous observation of an larger astorcytic response raised doubt about some alternatives: astrocytic Ca^{2+} chelation could lead a) to an increased synaptic glutamate release, and b) to a decreased release of GABA.

3. Clamping neurons to c.a. -40mV evoked a continuous AP firing. Under these conditions the local barrel stimulation induced a transient membrane hyperpolarization in which AP firing was interrupted (Fig.9). This occurred in the region of astrocytic Ca^{2+} response and was effectively prevented by astrocytic dialysis with BAPTA. The transient inhibition observed in control conditions could have been mediated directly by gliotransmission (release of GABA or adenosine) or indirectly by interneuron potentiation (astrocytic release of glutamate). Whatever the pathway, this result clearly pointed out that the consequence of gliotransmission upon barrel stimulation is a neuronal inhibition. Similarly, a transient post-burst inhibition was recently reported in hippocampus to depend on astrocytic Ca^{2+} elevation (Andersson & Hanse, 2010). A molecular pathway of gliotransmission in those circumstances was not described.

4. A single neuron was dialyzed with high chloride concentration (high $[Cl]_i$) through the patch pipette (Fig.13). This reproduced a physiological condition occurring in neurons at an early age (Uvarov et al., 2007), (Zhu et al., 2005). Upon such manipulation all $GABA_AR$-mediated responses in the patched neuron are excitatory. The advantage of this manipulation is that it impairs the GABAergic inhibition in the cell targeted for patch clamp while it avoids interfering with the rest of the brain network. Thus, it is probably the more useful and appropriate approach compared to drug application since GABAergic receptors are equally present on neurons and astrocytes. After such manipulation, the neuronal evoked response was increased similarly to the situation in which astrocytic Ca^{2+} was chelated. This not only supported the idea of a prominent GABAergic control of neuronal evoked response, it also suggested that a large part of the current elicited during the evoked response was carried by chloride. After dialysis with high $[Cl]_{I,}$ a neuron responded to the barrel stimulation in the same manner as when astrocytic Ca^{2+} was chelated. This supports the idea of an astrocytic-mediated inhibition which involves chloride-mediated currents. This is also in line with the idea that GABAergic inhibition is potentiated as a result of astrocytic Ca^{2+} elevation. A further experiment suggests this idea independently (Fig.11): somatic currents in neurons could be measured upon evoked response. We found that Ca^{2+} chelation in astrocytes suppressed an outward current. In agreement with previous experiments, we found that such current is largely carried by chloride.
5. We dialyzed a single neuron with high $[Cl]_i$ and chelated astrocytic Ca^{2+} (Fig.12). When the membrane potential was about -70 mV we observed

that the primary neuronal evoked response was not altered by the astrocytic dialysis. However, we observed “rebounds” of depolarization and AP firing for the following 10-15 seconds. This result further supports the idea of a Ca^{2+}-mediated astrocytic inhibition, but it ill-fits the concept of such mechanism being GABA-mediated. With high $[Cl]_{I,}$ single neurons were also depolarized via current injections and fired APs. The high $[Cl]_i$ prevented the transient inhibition upon barrel stimulation (Fig.9) before astrocytic Ca^{2+} chelation; however, neuronal firing was transiently suppressed upon local stimulation. This did not occur after astrocytic BAPTA dialysis, indicating that the transient inhibition of firing neurons upon local stimulation is mediated by chloride currents. It also suggests that there is a chloride-independent mechanism that transiently inhibits the neuronal firing during the seconds following the stimulation. Such mechanism depends on Ca^{2+}-mediated gliotransmission.

Five independent lines of experiments coherently suggested that astrocytic Ca^{2+} elevation causes neuronal inhibition. These results were obtained without pharmacological manipulations except the usage of BAPTA for astrocytic dialysis. Several of these results support the idea that chloride-mediated currents are the main carriers of such transient inhibition. However, chloride is not the only component of this mechanism. The results presented here are all in line with several previous publications (Kang et al. 1998), (Liu et al., 2004), (Kozlov et al., 2006), (Wang et al., 2006), (Schipke et al., 2008), (Lee et al., 2010). Some of them suggest possible pathways of gliotransmission: 1) Kang et al (1998) and Liu et al. (2004) show that Ca^{2+} elevation in astrocytes potentiates synaptic release of

GABA. According to these authors, this involves presynaptic AMPA or mGluR receptor activation. If this mechanism applies to our system, we could expect the gliotransmitter to be glutamate. 2) Serrano et al. (2006) shows that Ca^{2+}-dependent adenosine release causes heterosynaptic inhibition. If this were occurring in our situation, the primary gliotransmitter would be ATP or adenosine. 3) Koslov et al. 2006 and Lee et al. 2010 show that GABA can be directly released from astrocytes upon Ca^{2+} elevation. If the same happened in our system, the primary gliotransmitter would be GABA. Four out of five lines of our experiments suggest that the end component in the pathway of gliotransmission is GABA. In support of this theory, we observed in further experiments that pharmacological blockage of GABAR could reproduce the neuronal response increase as upon astrocytic Ca^{2+} chelation. The blockage of other possible upstream pathways of gliotransmission should also have similar effects.

Astrocyte-mediated inhibition and GABA-mediated inhibition (analogies)

Astrocytes respond to synchronous neuronal depolarization with a Ca^{2+} increase (Schipke et al., 2008).

In several lines of experiments, we showed that this leads in turn to neuronal inhibition. GABA appears to be involved in such inhibitory mechanism. This was clearly shown when we tested the effect of GABAergic blockers on the evoked neuronal response.

1) We focused on the stimulation paradigm as in Fig.3 and Fig. 6. Namely neurons were patched and held at their resting potential while the barrel was electrically stimulated. The same procedure was repeated upon application of GABAergic blockers. We remark that in our experiments the

flow of the medium through the bath chamber was held constant, in contrast to Schipke et al. 2008.

Blocking $GABA_A$ receptors with gabazine led to an increase in the amplitude of the neuronal evoked response during stimulation. Blocking $GABA_B$ receptors had little effect on the amplitude but prolonged the duration of the response (Fig.8). In combination, $GABA_A$ and $GABA_B$ receptor blockade mimicked the effects of astrocyte dialysis with BAPTA.

2) We blocked similarly $GABA_A$ and $GABA_B$ receptors upon tonic neuronal depolarization (Fig.9) and found that also in this respect the pharmacological blockage reproduced the astrocytic dialysis with BAPTA.
3) We finally measured the outward current evoked by barrel stimulation (Fig.14) and found that GABAergic blockage abolished such current as after astrocytic Ca^{2+} chelation.

These three experiments lead us to conclude that the final effector of astrocytic-mediated inhibition is actually GABA. This idea is reinforced by the fact that the blockage of $GABA_AR$ or $GABA_BR$ alone does not suffice in reproducing the effects of Ca^{2+} chelation, and that joint blockage of both receptor types is required (Fig.8). These findings are mostly suggestive of astrocytic-mediated interneuronal potentiation (Kang et al. 1998), (Liu et al., 2004) or astrocytic Ca^{2+}-mediated GABA release (Kozlov et al., 2006), (Lee et al., 2010). We nevertheless need to take in account that there could be other unrelated forms of gliotransmission reproducing the effect of GABAergic blockage. For this reason, we studied several other pathways of gliotransmission which were described in the past accounting for neuromodulation. These pathways will be discussed later.

Location of $GABA_A$ and $GABA_B$ receptors

GABA receptors are not just part of the neuronal repertoire but are also functionally present on astrocytes (Bowman & Kimelberg, 1984), (Kettenmann et al., 1984), (Kang et al. 1998), (Liu et al., 2000), (Serrano et al., 2006). Therefore, we cannot exclude that GABAergic blockers had a mixed effect. Part of their action was, however, clearly directed to the studied neurons. Under control conditions, the reversal potential of the stimulus-induced currents was at about -50mV. This was close to the imposed Cl^- equilibrium potential (-65 mV). Dialysis of neurons with high chloride concentration (E_{Cl} ~ 0 mV) shifted the reversal potential of such current to about 0 mV. This revealed that the stimulus-induced current in control conditions was largely carried by chloride. Given the reversal potential of such current and the sensitivity to gabazine we conclude that $GABA_AR$ are located on the neuron under study. $GABA_BR$ was also a component in the inhibitory mechanism limiting the barrel evoked response. $GABA_BR$ are metabotropic receptors that can act at both the pre- and postsynaptic membrane. The postsynaptic action is mediated by a specific family of K^+ channels: the G-protein-gated inwardly rectifying K^+ (GIRK/Kir3) channels (Misgeld, Bijak & Jarolimek, 1995), (Padgett & Slesinger, 2010). The GIRK kind of channel, coupled to $GABA_BR$, can vary between cell types and brain regions (Koyrakh et al., 2005). We found that $GABA_BR$ blockade prolonged the depolarization phase. If such an effect was postsynaptic, this would imply that in our system GIRK channels controlled the membrane repolarization. The presynaptic mechanism is instead based on a G-protein controlling the presynaptic Ca^{2+} currents, hence the synaptic release (Deisz et al., 1997), (Brown & Sihra, 2008). This controls the

neuronal excitability in rodents' neocortex (Deisz, 2002). If $GABA_B$ receptors were presynaptic, this could explain why the effect of baclofen on the "low $[Cl]_i$" neurons was limited (Fig.13): even the direct blockage of glutamate receptor had a negligible effect on the evoked response (Fig.14) Thus, the decreased release of glutamate due to presynaptic $GABA_BR$ activation could not further suppress the evoked response. The effect of baclofen on "high $[Cl]_i$" neurons was by contrast prominent, because in such conditions $GABA_AR$ provides the main drive for neuronal excitation. A presynaptic decrease of GABA release would therefore have the effect of decreasing the neuronal evoked response. This is a speculation which could be validated by the use of AMPA and NMDA receptor blockers. However, we did not proceed with further experiments in such directions.

We also observed that the ePSCs frequency was increased upon astrocytic BAPTA dialysis (Fig.15). This would conform to the idea of presynaptic $GABA_B$ localization. Thus, our results support both pre- and postsynaptic $GABA_BR$ localization while not ruling out either of the two other possibilities. Furthermore, we need to consider the possibility for GABAR to be located on the astrocytic membrane (Kang et al. 1998), (Liu et al., 2000), (Serrano et al., 2006). In such a scenario, the GABAergic inhibition of neuronal evoked response might follow a very complicated pathway. It could, for instance, reduce the neuronal evoked response through direct $GABA_A$ activation. At the same time, it might act through autocrine $GABA_B$ receptors and cause the astrocytic release of other gliotransmitters which would in turn inhibit the neuronal synaptic release.

In summary, astrocytic Ca^{2+} chelation was largely reproduced by $GABA_A$ and $GABA_B$ receptor blockade. If it is likely for $GABA_A$ receptors to be located on the postsynaptic neuronal membrane, it remains to be shown in which position the

$GABA_B$ receptors are involved in our model. Based on our own results and on previous literature, we cannot exclude them from being neuronal, pre-or post synaptic, or even astrocytic, and mediating a complex autocrine loop of neuromodulation.

Other receptors possibly involved in the gliotransmission leading to GABAergic inhibition

Glutamate

Several authors report glutamate as an important gliotransmitter released from astrocytes through various mechanisms (Parpura et al., 1994), (Szatkowski et al., 1990), (Kimelberg et al., 1990), (Duan et al., 2003), (Ye et al., 2003), (Warr et al., 1999).

Kang et al (1998) provided evidence that interneurons, when repeatedly stimulated, trigger $GABA_B$-mediated Ca^{2+} responses in astrocytes. This in turn transiently potentiates inhibitory postsynaptic currents in CA1 pyramidal neurons. Such potentiation was abolished by astrocyte BAPTA dialysis so that with those experiments Kang provided evidence for astrocytic Ca^{2+}-mediated potentiation of interneurons. Our experiments could possibly be explained by such gliotransmission pathways or by the interneurons that play a strong role in limiting the barrel excitation (Swadlow, 2002). If so, we would expect AMPA presynaptic receptors to be activated by glutamate. Unfortunately, we did not find a straightforward strategy to test this hypothesis. We plan, however, to characterize the same type of gliotransmission by targeting interneurons. In such a context,

the stimulation of interneurons upon astrocytic dialysis could reveal how presynaptic release of GABA is affected.

Several metabotropic receptors are involved in the astrocytic calcium responses to neurons (Verkhratsky & Kettenmann, 1996), (Verkhratsky, 2006), (Verkhratsky et al., 1998). Astrocytic release of glutamate was shown, on the other hand, to increase inhibitory transmission via neuronal metabotropic receptor stimulation (Liu et al., 2004). mGluRs were involved in barrel cortex inducing astrocytic Ca^{2+} responses upon whisker stimulation (Wang *et al.* 2006). All the same, the mGluR blockage was not reported to sensibly alter the local neuronal field potential. Given the higher sensibility of our recording method, we decided to test the involvement of mGluR in the barrel evoked responses that could have been previously missed. Similar to Wang et al. (2006), we observed that *trans*-ACPD directly induced astrocytic Ca^{2+} responses. When in those conditions the barrel was locally stimulated, we did not detect changes in the neuronal evoked response, except for a few neurons which fired a tail of APs during the repolarization phase. *trans*-ACPD did not evoke an additional astrocytic calcium response on top of the one evoked by electrical stimulation. This could explain why it did not modulate the neuronal evoked response. We expected in contrast that the application of LY367385 and MPEP (mGluR blockers) would impair the astrocytic Ca^{2+} elevation and thus affect the neuronal evoked response. This would have revealed the relevance of glutamatergic gliotransmission to our system. The two blockers, however, failed to affect the astrocytic Ca^{2+} increase. They nevertheless slightly prolonged the duration of the neuronal evoked response. In conclusion, mGluRs and glutamatergic gliotransmission may participate in the neuromodulation of barrel cortex neurons, but this is not the only

or the major mechanism accounting for GABAergic potentiation. The failure of astrocytic modulation by these mGluR blockers is not surprising as astrocytes are activated by multiple substances as glutamate (Verkhratsky et al., 1998), (Seifert & Steinhauser, 1995) (Lalo et al., 2006), (Lalo et al., 2008), (Luque & Richards, 1995), (Mathyas et al. 2001), GABA and glycine (Bowman & Kimelberg, 1984), (Kettenmann et al., 1984) and ATP (Cotrina et al., 2000).

ATP/adenosine

ATP and adenosine based gliotransmission accounts for a wide variety of neuromodulatory effects in the brain (Gourine et al., 2010), (Pascual et al., 2005), (Halassa et al., 2007), (Halassa et al., 2010). After extracellular degradation from ATP, adenosine has been reported to play a key role in modulating the neuronal excitability. This is relevant for several aspects of brain network physiology (Halassa et al., 2007), (Halassa et al., 2010) (Serrano et al. 2006). For instance, we hypothesized that adenosine could be involved in the control of heterosynaptic inhibition as described for the hippocampus (Serrano et al. 2006). This could similarly account for columnar propagation of neuronal inputs between the barrel neurons. If such was the pathway of gliotransmission in our system, we would predict that the blockage of P1A receptors would mimic the effect of local astrocytic Ca^{2+} chelation and those of GABAergic blockage. Previous data showing the effect of Suramine and CPT on the size of astrocytic Ca^{2+} response (Schipke *et al.* 2008) support the involvement of adenosine in this system.

We instead failed to observe any effect on neurons after CPT application. In a separate set of experiments we found that CPT was inefficient in increasing the

astrocytic Ca^{2+} response. This was in contrast to what Schipke et al (2008) observed Upon further investigation, we found that the reason for such a discrepancy was probably in the protocols for drug application. Contrary to the present experiments, Schipke et al (2008) stopped the flow of artificial cerebrospinal fluid (ACSF) through the recording chamber during the drug application. We found that stopping the superfusion lead by itself to large astrocytic Ca^{2+} responses. We therefore conclude that CPT application in barrel cortex neither affects the neuronal nor the astrocytic-evoked response, and heterosynaptic inhibition through A_1 receptors is not a pathway of gliotransmission that applies to our system. Considering the possible effects of ATP/adenosine release in respect to their effect on a single receptor would be an underestimation. The variety of receptors for such molecules in the brain is vast (Burnstock et al., 2011). Possible impairment of ATP release could also have autocrine effects on the astrocytes themselves (Cotrina et al., 2000) with potential repercussions on the release of other gliotransmitters. For this purpose, the laboratory recently launched a project for the characterization of purinergic effects on astrocytic Ca^{2+} elevation and neuronal modulation in barrel cortex. The findings will help to better understand this potential pathway of neuromodulation in our system.

D-Serine

D-serine is a gliotransmitter co-released by astrocytes together with glutamate (Mothet et al., 2005) and could be involved in neuromodulation in our system. Long-term potentiation in the hippocampus requires D-Serine and a functional Ca^{2+} astrocytic elevation (Henneberger et al., 2010). Hennenberger and co-

workers (2010) have shown that D-Serine release from astrocytes is Ca^{2+}-dependent and plays a pivotal role in hippocampal plasticity. D-Serine is a modulator of glutamate on NMDA receptors. Although plasticity is not induced in our model, we speculated that if this amino acid played any role in the cortex this could be highlighted by the selective degradation of D-Serine. We therefore applied D-amino acid oxidase (D-AAO) to the brain slices before our experiments to oxidize the D-Serine amino terminal. In these conditions, we observed no alterations in the barrel evoked response. Hence, D-Serine was not involved in our model. A point of concern was raised concerning the possible D-AAO contamination. The product commercially available from Sigma was supposed to specifically target D-Serine but was found to contain an undetermined amount of D-*aspartate* oxidase (Shleper, Kartvelishvily & Wolosker, 2005). Such contamination does not affect our results. All the same, we highlight such contamination since this is not reported on the product information by Sigma although the evidence of contamination has existed since 2005. If a system is tested with NMDA application, D-AAO will induce a decreased response which is largely an artefact.

Glycine

We assumed that, even as minor component, glycinergic neurons are present in the cortex (Zeilhofer et al., 2005). Glycine receptors are permeable to chloride, so they could play a relevant role in our model. To test this, we recorded the barrel evoked responses upon strychnine application. We failed, however, to observe a significant modulation of the neuronal evoked response in such conditions, except

for a modest shortening of the repolarization after stimulus delivery. This ruled out glycine from the list of the neuromodulators possibly involved in our system.

In summary, our aggregate data leads us to conclude that none of the gliotransmitters studied in previous publications had a major role in our system. Even so it appears that in such contexts Ca^{2+} chelation in astrocytes leads to the impairment of neuronal inhibition and this is likely to be mediated in turn by the impairment of $GABA_A$Rs and $GABA_B$Rs. Our results therefore strongly suggest that astrocytes might be directly involved in the control of barrel cortex neurons through the release of GABA. The possibility of such Ca^{2+} dependent gliotransmission has already been demonstrated in two other contexts (Kozlov et al., 2006), (Lee et al., 2010). Lee et al (2010) showed that a glial mechanism for GABA release is the opening of the Ca^{2+}-gated chloride channel Bestrophin. This, in turn, accounts for a tonic inhibition of cerebellar neurons. Further experiments will reveal whether such a mechanism accounts for GABAergic gliotransmission in our system as well.

Perspectives

ePSC frequency and long-term modulation

We found that ePSC frequency is upregulated upon astrocytic Ca^{2+} chelation. This supports our data about an inhibitory role of astrocytes. It also leads us to question whether astrocytic inhibition acts on neurons through an acute mechanism. Alternatively, a slow mechanism might in the long term condition the network excitability (Stellwagen & Malenka, 2006), (Lee et al., 2010). Since it was recently shown that GABA is tonically released from astrocytes (Lee et al., 2010), this could count in our system as well. Another possible pathway through which astrocytes might control the ambient GABA and modulate neuronal excitability is by reverse transporter activity. Astrocytes are known to express GABA transporters (GATs) that can contribute up to 20% of GABA uptake from the extracellular space (Schousboe et al. 1977; Hertz et al. 1978; Schousboe, 2000). Modulation in GABA uptake or the reverse transport of GABA might be a potential mechanism for the GABAergic inhibition mediated by astrocytes (Heja et al. 2009; Park et al. 2009). Our findings support the latter speculation, specifically the prolonged application (over 1 hr) of SNAP 5114, a selective inhibitor of glial GABA transport (GAT 2/3) caused an increased neuronal evoked response similar to astrocytic BAPTA dialysis. Since glutamate uptake triggers the release of GABA from astrocytes (Heja et al., 2009), we reasoned that Ca^{2+} elevation might affect this process. However, SNAP 5114 is effective only after a prolonged incubation. This suggests that the block of GAT 2/3 might increase the neuronal excitability through a long-term conditioning of the network. We also observed that frequent

stimulation (every 60 s) overcame the SNAP5114-mediated increase of neuronal evoked response with a mechanism of depression. This implies the presence of other parallel inhibitory mechanisms but does not provide any indication for their nature. In this respect, it would be interesting to verify whether the evoked response depression upon frequent stimulation depends on astrocytic Ca^{2+} elevation. It would also be interesting to observe whether other blockers that failed to modulate the neuronal evoked response would become effective upon a longer incubation period. This would indicate that a tonic control rather than a transient inhibition occurs in the barrel cortex. It would also imply that the transient Ca^{2+} elevation upon evoked response is not the main trigger of the glial-dependent neuronal inhibition as observed in our study.

Increased ePSC frequency and the effects of SNAP 5114 long-term incubation suggest that gliotransmitters could be accounting for a tonic inhibition of the barrel cortex neurons. Remarkably, both results are compatible with the possibility of astrocytic release of GABA. Particularly the increased ePSC frequency can be explained by a decreased presynaptic $GABA_BR$ stimulation upon astrocytic Ca^{2+} chelation. How could the dialysis with BAPTA affect gliotransmission in the absence of an evoked response implying Ca^{2+} elevation? We speculate that microdomains of spontaneous Ca^{2+} elevation might be involved in tonic gliotransmission. Ca^{2+} microdomains have been recently characterized in astrocytes (Shigetomi et al., 2010). The detection of such microdomains with conventional Ca^{2+} sensors fails, but the authors report that microdomains are sensitive to BAPTA dialysis. It will be interesting to verify whether microdomains of Ca^{2+} elevation are occurring in barrel cortex astrocytes and if they account for

gliotransmission. Determining to what extent the GABAergic control of barrel cortex neurons is controlled by a tonic mechanism is also an attractive target for future experiments.

Interneurons

Previous reports showed that astrocytes are either capable of directly inhibiting neurons through tonic GABA release (Kozlov *et al*,2006, Lee et al. 2010) or indirectly potentiating the release of GABA from interneurons (Kang et al. 1998). The measurement of evoked and spontaneous neuronal activity in interneurons and the measurement of inhibitory post-synaptic currents (iPSCs) are currently under way. With these experiments, we will assess whether the gliotransmission that mediates GABAergic inhibition in barrel cortex is a direct pathway or involves interneuronal potentiation.

Gap junctions, potassium buffering and calcium chelation

Is it possible that the dialysis of the astrocytic syncytium with BAPTA altered the coupling between glial cells? We observed in BAPTA dialysis that the overall spreading of our intracellular solution was efficient. In c.a. one hour the dye, showing the degree of coupling visibly spread to c.a. 10 neighboring astrocytes thus not grossly impairing astrocytic coupling by the calcium chelation. We observed nevertheless that, after dialysis with BAPTA, the dye showing the degree of coupling did not reach some of the neighboring cells regardless of their proximity from the primary dialyzed astrocyte (Fig.4). Similar results were also obtained with experiments of Ca^{2+} imaging. The apparent uncoupling could be due to the fact that some cells were already not coupled or because their coupling

was interrupted by the tissue slicing. It is, however, tempting to speculate that some degree of coupling reduction may be caused by the intracellular calcium chelation in astrocytes. This needs to be confirmed in further experiments.

The local stimulation applied in our model evoked a prominent and synchronous neuronal depolarization and AP firing. Thus, we need to take in account that our stimulating conditions might have caused a prominent local potassium increase. We speculate that the increased neuronal excitability may be the consequence of an impairment of astrocytic spatial potassium buffering (Kofuji & Newman, 2004). Such a mechanism is relevant in epilepsy where the neuronal excitability is increased by both a decreased expression of potassium inward rectifier channels (Kir) or by decreased gap junctional coupling (for review see (Seifert et al., 2010). So far we observed that the steady state (potassium) currents evoked in neurons (Fig.11) upon astrocytic Ca^{2+} chelation were comparable to control (statistic not reported). This at least suggests that the local potassium concentration was not sensibly changed in unstimulated slices. The reduction of outward currents during the evoked responses might instead suggest the impaired potassium buffering upon intense stimulation. Against this, our results suggest that the main current-carrier during the evoked response is chloride. The quantification of potassium components in such evoked current needs to be addressed with further experiments. Our data, however, do not suggest the impairment of potassium buffering after BAPTA dialysis. Another consequence of the potential redistribution in the gap junctional coupling might be the change in astrocytic release of glutamate (Ye et al., 2003). In this respect the consequence of a decreased release of glutamate might affect the efficiency of interneuronal release of GABA

as discussed above. The arrangement of astrocytic syncytia in vertical columns aligned within the single barrels (Houades et al. 2008) suggests the importance of the pattern of astrocytic coupling in the somatosensory cortex. For these reasons, an accurate study of gap junctional coupling in relation to astrocytic BAPTA dialysis would be an interesting subject for future studies.

Possible functional roles of gliotransmission in barrel cortex

The context of gliotransmission we described is certainly very peculiar: the shape of the astrocytic calcium responses and the underlying neuronal activity suggest that astrocytes and gliotransmission in the juvenile barrel cortex might constrain the large and synchronous network activity in the barrel columns. It is tempting to speculate that such gliotransmission could be an effective mechanism preventing some whisking pattern (Wang et al. 2006) to cause an excessive excitability in the juvenile brain or preventing the large activity of a single barrel to spread to the neighboring columns.

In future experiments the measurement of neuronal evoked responses at progressive stimulation intensities (or frequencies) might reveal the threshold of neuronal activity required for an efficient astrocytic recruitment. The measurement of neuronal activity outside the stimulated column and after local BAPTA dialysis might reveal the role of gliotransmission in the spatial control of brain network excitability.

CONCLUSION

This study shows clearly that astrocytes control GABAergic inhibition of neurons in the mouse barrel cortex. A prominent neuronal activity was required to activate astrocytic columnar Ca^{2+} responses in barrel cortex. Astrocytic Ca^{2+} chelation caused in turn an increased neuronal excitability. Astrocytes therefore inhibit barrel cortex neurons in a Ca^{2+}-dependent fashion. Whatever the molecular pathway, several lines of experiments indicate that such astrocytic-mediated inhibition involves GABA, although other gliotransmitters such as glutamate could contribute to the mechanism. Whether astrocytes directly inhibit the barrel cortex neurons or they act indirectly potentiating, for instance, the interneuronal activity is still to be verified. Both alternatives could coexist.

Glial GABA transporters could be involved in the mechanism of gliotransmission and it is possible for part of the astrocytic-mediated inhibition to occur through tonic gliotransmitter release. In conclusion, astrocytes control neuronal inhibition in the barrel cortex through Ca^{2+}-dependent gliotransmission involving $GABA_A$ and $GABA_B$ receptors. The exact underlying molecular mechanism will be resolved in future experiments.

ACKNOWLEDGMENTS

We would like to thank Prof. Dirk Feldmeyer (Forschungzentrum Juelich, Germany), Prof. Joachim Lübke (Juelich, Germany), Prof. Alexej Verkhratsky, (Manchester, UK) Prof. Dr. Christian Steinhäuser (Bonn, Germany), Dr. Christiane Nolte (Berlin, Germany), Prof. Philip Haydon, (Boston, USA), Prof. Rosemary Grantyn (Berlin, Germany) and Prof. Rudolf Deisz (Berlin, Germany) for their critical comments and helpful discussion. We would also like to thank Prof. Frank Kirchhoff (Homburg / Saar, Germany) for providing the mRFP/GFAP mouse strain and Dr. Karljin Van Aerde (Juelich, Germany) for the custom-made “IGORpro” function kindly provided for neuronal characterization.

FUNDING

This work was supported by the Deutsche Forschungsgemeinschaft (SPP 1172).

BIBLIOGRAPHY

AGMON, A. & CONNORS, B. W. (1991). Thalamocortical responses of mouse somatosensory (barrel) cortex in vitro. *Neuroscience* **41,** 365-79.

AGMON, A. & CONNORS, B. W. (1992). Correlation between intrinsic firing patterns and thalamocortical synaptic responses of neurons in mouse barrel cortex. *J Neurosci* **12,** 319-29.

AGULHON, C., FIACCO, T. A. & MCCARTHY, K. D. (2010). Hippocampal short- and long-term plasticity are not modulated by astrocyte Ca2+ signaling. *Science* **327,** 1250-4.

ALLEN, N. J. & BARRES, B. A. (2005). Signaling between glia and neurons: focus on synaptic plasticity. *Curr Opin Neurobiol* **15,** 542-8.

ANDERSSON, M. & HANSE, E. (2010). Astrocytes impose postburst depression of release probability at hippocampal glutamate synapses. *J Neurosci* **30,** 5776-80.

ANGULO, M. C., LE MEUR, K., KOZLOV, A. S., CHARPAK, S. & AUDINAT, E. (2008). GABA, a forgotten gliotransmitter. *Prog Neurobiol* **86,** 297-303.

ARAQUE, A., LI, N., DOYLE, R. T. & HAYDON, P. G. (2000). SNARE protein-dependent glutamate release from astrocytes. *J Neurosci* **20,** 666-73.

ARAQUE, A., MARTIN, E. D., PEREA, G., ARELLANO, J. I. & BUNO, W. (2002). Synaptically released acetylcholine evokes Ca2+ elevations in astrocytes in hippocampal slices. *J Neurosci* **22,** 2443-50.

ARAQUE, A. & PEREA, G. (2004). Glial modulation of synaptic transmission in culture. *Glia* **47,** 241-8.

ARAQUE, A., SANZGIRI, R. P., PARPURA, V. & HAYDON, P. G. (1998). Calcium elevation in astrocytes causes an NMDA receptor-dependent increase in the frequency of miniature synaptic currents in cultured hippocampal neurons. *J Neurosci* **18,** 6822-9.

ARCUINO, G., LIN, J. H., TAKANO, T., LIU, C., JIANG, L., GAO, Q., KANG, J. & NEDERGAARD, M. (2002). Intercellular calcium signaling mediated by point-source burst release of ATP. *Proc Natl Acad Sci U S A* **99,** 9840-5.

BACCI, A., SANCINI, G., VERDERIO, C., ARMANO, S., PRAVETTONI, E., FESCE, R., FRANCESCHETTI, S. & MATTEOLI, M. (2002). Block of glutamate-glutamine cycle between astrocytes and neurons inhibits epileptiform activity in hippocampus. *J Neurophysiol* **88,** 2302-10.

BARDONI, R., GHIRRI, A., ZONTA, M., BETELLI, C., VITALE, G., RUGGIERI, V., SANDRINI, M. & CARMIGNOTO, G. (2010). Glutamate-mediated astrocyte-to-neuron signalling in the rat dorsal horn. *J Physiol* **588,** 831-46.

BEATTIE, E. C., STELLWAGEN, D., MORISHITA, W., BRESNAHAN, J. C., HA, B. K., VON ZASTROW, M., BEATTIE, M. S. & MALENKA, R. C. (2002). Control of synaptic strength by glial TNFalpha. *Science* **295,** 2282-5.

BEIERLEIN, M., GIBSON, J. R. & CONNORS, B. W. (2003). Two dynamically distinct inhibitory networks in layer 4 of the neocortex. *J Neurophysiol* **90,** 2987-3000.

BEKAR, L. K., HE, W. & NEDERGAARD, M. (2008). Locus coeruleus alpha-adrenergic-mediated activation of cortical astrocytes in vivo. *Cereb Cortex* **18,** 2789-95.

BERGLES, D. E., JABS, R. & STEINHAUSER, C. (2010). Neuron-glia synapses in the brain. *Brain Res Rev* **63,** 130-7.

BEZZI, P., CARMIGNOTO, G., PASTI, L., VESCE, S., ROSSI, D., RIZZINI, B. L., POZZAN, T. & VOLTERRA, A. (1998). Prostaglandins stimulate calcium-dependent glutamate release in astrocytes. *Nature* **391,** 281-5.

BEZZI, P., GUNDERSEN, V., GALBETE, J. L., SEIFERT, G., STEINHAUSER, C., PILATI, E. & VOLTERRA, A. (2004). Astrocytes contain a vesicular compartment that is competent for regulated exocytosis of glutamate. *Nat Neurosci* **7,** 613-20.

BOWMAN, C. L. & KIMELBERG, H. K. (1984). Excitatory amino acids directly depolarize rat brain astrocytes in primary culture. *Nature* **311,** 656-9.

BROWN, D. A. & SIHRA, T. S. (2008). Presynaptic signaling by heterotrimeric G-proteins. *Handb Exp Pharmacol***,** 207-60.

BURNSTOCK, G., FREDHOLM, B. B. & VERKHRATSKY, A. (2011). Adenosine and ATP receptors in the brain. *Curr Top Med Chem* **11,** 973-1011.

CHAGNAC-AMITAI, Y. & CONNORS, B. W. (1989). Synchronized excitation and inhibition driven by intrinsically bursting neurons in neocortex. *J Neurophysiol* **62,** 1149-62.

CHARLES, A. C., MERRILL, J. E., DIRKSEN, E. R. & SANDERSON, M. J. (1991). Intercellular signaling in glial cells: calcium waves and oscillations in response to mechanical stimulation and glutamate. *Neuron* **6,** 983-92.

CORNELL-BELL, A. H., FINKBEINER, S. M., COOPER, M. S. & SMITH, S. J. (1990). Glutamate induces calcium waves in cultured astrocytes: long-range glial signaling. *Science* **247,** 470-3.

COTRINA, M. L., LIN, J. H., LOPEZ-GARCIA, J. C., NAUS, C. C. & NEDERGAARD, M. (2000). ATP-mediated glia signaling. *J Neurosci* **20,** 2835-44.

DEFELIPE, J. (1999). Chandelier cells and epilepsy. *Brain* **122 (Pt 10),** 1807-22.

DEFELIPE, J. (2002). Cortical interneurons: from Cajal to 2001. *Prog Brain Res* **136,** 215-38.

DEFELIPE, J., HENDRY, S. H., HASHIKAWA, T., MOLINARI, M. & JONES, E. G. (1990). A microcolumnar structure of monkey cerebral cortex revealed by immunocytochemical studies of double bouquet cell axons. *Neuroscience* **37,** 655-73.

DEISZ, R. A. (2002). Cellular mechanisms of pharmacoresistance in slices from epilepsy surgery. *Novartis Found Symp* **243,** 186-99; discussion 199-206, 231-5.

DEISZ, R. A., BILLARD, J. M. & ZIEGLGANSBERGER, W. (1997). Presynaptic and postsynaptic GABAB receptors of neocortical neurons of the rat in vitro: differences in pharmacology and ionic mechanisms. *Synapse* **25,** 62-72.

DEITMER, J. W. & ROSE, C. R. (2010). Ion changes and signalling in perisynaptic glia. *Brain Res Rev* **63,** 113-29.

DEITMER, J. W. & STEINHAUSER, C. (2010). Synaptic processes-The role of glial cells. Preface. *Brain Res Rev* **63,** 1.

DOMBECK, D. A., KHABBAZ, A. N., COLLMAN, F., ADELMAN, T. L. & TANK, D. W. (2007). Imaging large-scale neural activity with cellular resolution in awake, mobile mice. *Neuron* **56,** 43-57.

DUAN, S., ANDERSON, C. M., KEUNG, E. C., CHEN, Y. & SWANSON, R. A. (2003). P2X7 receptor-mediated release of excitatory amino acids from astrocytes. *J Neurosci* **23,** 1320-8.

FAM, S. R., GALLAGHER, C. J., KALIA, L. V. & SALTER, M. W. (2003). Differential frequency dependence of P2Y1- and P2Y2- mediated Ca 2+ signaling in astrocytes. *J Neurosci* **23,** 4437-44.

FELDMEYER, D., EGGER, V., LUBKE, J. & SAKMANN, B. (1999). Reliable synaptic connections between pairs of excitatory layer 4 neurones within a single 'barrel' of developing rat somatosensory cortex. *J Physiol* **521 Pt 1,** 169-90.

FELDMEYER, D., LUBKE, J. & SAKMANN, B. (2006). Efficacy and connectivity of intracolumnar pairs of layer 2/3 pyramidal cells in the barrel cortex of juvenile rats. *J Physiol* **575,** 583-602.

FELDMEYER, D., LUBKE, J., SILVER, R. A. & SAKMANN, B. (2002). Synaptic connections between layer 4 spiny neurone-layer 2/3 pyramidal cell pairs in juvenile rat barrel cortex: physiology and anatomy of interlaminar signalling within a cortical column. *J Physiol* **538,** 803-22.

FELDMEYER, D., ROTH, A. & SAKMANN, B. (2005). Monosynaptic connections between pairs of spiny stellate cells in layer 4 and pyramidal cells in layer 5A indicate that lemniscal and paralemniscal afferent pathways converge in the infragranular somatosensory cortex. *J Neurosci* **25,** 3423-31.

FELLIN, T., PASCUAL, O., GOBBO, S., POZZAN, T., HAYDON, P. G. & CARMIGNOTO, G. (2004). Neuronal synchrony mediated by astrocytic glutamate through activation of extrasynaptic NMDA receptors. *Neuron* **43,** 729-43.

FIACCO, T. A., AGULHON, C., TAVES, S. R., PETRAVICZ, J., CASPER, K. B., DONG, X., CHEN, J. & MCCARTHY, K. D. (2007). Selective stimulation of astrocyte calcium in situ does not affect neuronal excitatory synaptic activity. *Neuron* **54,** 611-26.

FIACCO, T. A. & MCCARTHY, K. D. (2004). Intracellular astrocyte calcium waves in situ increase the frequency of spontaneous AMPA receptor currents in CA1 pyramidal neurons. *J Neurosci* **24,** 722-32.

FOX, K. (2008). *Barrel Cortex*. Cambridge University Press, Cambridge, United Kingdom.

GALLAGHER, C. J. & SALTER, M. W. (2003). Differential properties of astrocyte calcium waves mediated by P2Y1 and P2Y2 receptors. *J Neurosci* **23,** 6728-39.

GOBEL, W., KAMPA, B. M. & HELMCHEN, F. (2007). Imaging cellular network dynamics in three dimensions using fast 3D laser scanning. *Nat Methods* **4,** 73-9.

GODDARD, G. V., MCINTYRE, D. C. & LEECH, C. K. (1969). A permanent change in brain function resulting from daily electrical stimulation. *Exp Neurol* **25,** 295-330.

GOMEZ-GONZALO, M., LOSI, G., CHIAVEGATO, A., ZONTA, M., CAMMAROTA, M., BRONDI, M., VETRI, F., UVA, L., POZZAN, T., DE CURTIS, M., RATTO, G. M. & CARMIGNOTO, G. (2010). An excitatory loop with astrocytes contributes to drive neurons to seizure threshold. *PLoS Biol* **8,** e1000352.

GOSEJACOB, D., DUBLIN, P., BEDNER, P., HUTTMANN, K., ZHANG, J., TRESS, O., WILLECKE, K., PFRIEGER, F., STEINHAUSER, C. & THEIS, M. (2011). Role of astroglial connexin30 in hippocampal gap junction coupling. *Glia* **59,** 511-9.

GOURINE, A. V., KASYMOV, V., MARINA, N., TANG, F., FIGUEIREDO, M. F., LANE, S., TESCHEMACHER, A. G., SPYER, K. M., DEISSEROTH, K. & KASPAROV, S. (2010). Astrocytes control breathing through pH-dependent release of ATP. *Science* **329,** 571-5.

GROSCHE, J., MATYASH, V., MOLLER, T., VERKHRATSKY, A., REICHENBACH, A. & KETTENMANN, H. (1999). Microdomains for neuron-glia interaction: parallel fiber signaling to Bergmann glial cells. *Nat Neurosci* **2,** 139-43.

GUTHRIE, P. B., KNAPPENBERGER, J., SEGAL, M., BENNETT, M. V., CHARLES, A. C. & KATER, S. B. (1999). ATP released from astrocytes mediates glial calcium waves. *J Neurosci* **19,** 520-8.

GUTNICK, M. J., CONNORS, B. W. & PRINCE, D. A. (1982). Mechanisms of neocortical epileptogenesis in vitro. *J Neurophysiol* **48,** 1321-35.

HALASSA, M. M., DAL MASCHIO, M., BELTRAMO, R., HAYDON, P. G., BENFENATI, F. & FELLIN, T. (2010). Integrated brain circuits: neuron-astrocyte interaction in sleep-related rhythmogenesis. *ScientificWorldJournal* **10,** 1634-45.

HALASSA, M. M., FELLIN, T., TAKANO, H., DONG, J. H. & HAYDON, P. G. (2007). Synaptic islands defined by the territory of a single astrocyte. *J Neurosci* **27,** 6473-7.

HALASSA, M. M., FLORIAN, C., FELLIN, T., MUNOZ, J. R., LEE, S. Y., ABEL, T., HAYDON, P. G. & FRANK, M. G. (2009). Astrocytic modulation of sleep homeostasis and cognitive consequences of sleep loss. *Neuron* **61,** 213-9.

HALASSA, M. M. & HAYDON, P. G. (2010). Integrated brain circuits: astrocytic networks modulate neuronal activity and behavior. *Annu Rev Physiol* **72,** 335-55.

HARRIS, E. & STEWART, M. (2001). Propagation of synchronous epileptiform events from subiculum backward into area CA1 of rat brain slices. *Brain Res* **895,** 41-9.

HEJA, L., BARABAS, P., NYITRAI, G., KEKESI, K. A., LASZTOCZI, B., TOKE, O., TARKANYI, G., MADSEN, K., SCHOUSBOE, A., DOBOLYI, A., PALKOVITS, M. & KARDOS, J. (2009). Glutamate uptake triggers transporter-mediated GABA release from astrocytes. *PLoS One* **4,** e7153.

HELMSTAEDTER, M., SAKMANN, B. & FELDMEYER, D. (2009). L2/3 interneuron groups defined by multiparameter analysis of axonal projection, dendritic geometry, and electrical excitability. *Cereb Cortex* **19,** 951-62.

HENNEBERGER, C., PAPOUIN, T., OLIET, S. H. & RUSAKOV, D. A. (2010). Long-term potentiation depends on release of D-serine from astrocytes. *Nature* **463,** 232-6.

HIRASE, H., QIAN, L., BARTHO, P. & BUZSAKI, G. (2004). Calcium dynamics of cortical astrocytic networks in vivo. *PLoS Biol* **2,** E96.

HIRRLINGER, P. G., SCHELLER, A., BRAUN, C., QUINTELA-SCHNEIDER, M., FUSS, B., HIRRLINGER, J. & KIRCHHOFF, F. (2005). Expression of reef coral fluorescent proteins in the central nervous system of transgenic mice. *Mol Cell Neurosci* **30,** 291-303.

HOUADES, V., KOULAKOFF, A., EZAN, P., SEIF, I. & GIAUME, C. (2008). Gap junction-mediated astrocytic networks in the mouse barrel cortex. *J Neurosci* **28,** 5207-17.

HUANG, Y. H. & BERGLES, D. E. (2004). Glutamate transporters bring competition to the synapse. *Curr Opin Neurobiol* **14,** 346-52.

KANG, J., JIANG, L., GOLDMAN, S. A. & NEDERGAARD, M. (1998). Astrocyte-mediated potentiation of inhibitory synaptic transmission. *Nat Neurosci* **1,** 683-92.

KELLER, A. & WHITE, E. L. (1987). Synaptic organization of GABAergic neurons in the mouse SmI cortex. *J Comp Neurol* **262,** 1-12.

KETTENMANN, H. & B.R., R. (2004). Neuroglia. *Oxford University press, New York*.

KETTENMANN, H., BACKUS, K. H. & SCHACHNER, M. (1984). Aspartate, glutamate and gamma-aminobutyric acid depolarize cultured astrocytes. *Neurosci Lett* **52,** 25-9.

KHIRUG, S., HUTTU, K., LUDWIG, A., SMIRNOV, S., VOIPIO, J., RIVERA, C., KAILA, K. & KHIROUG, L. (2005). Distinct properties of functional KCC2 expression in immature mouse hippocampal neurons in culture and in acute slices. *Eur J Neurosci* **21,** 899-904.

KIMELBERG, H. K., GODERIE, S. K., HIGMAN, S., PANG, S. & WANIEWSKI, R. A. (1990). Swelling-induced release of glutamate, aspartate, and taurine from astrocyte cultures. *J Neurosci* **10,** 1583-91.

KIRCHHOFF, F. (2010). Neuroscience. Questionable calcium. *Science* **327,** 1212-3.

KIRMSE, K., KIRISCHUK, S. & GRANTYN, R. (2009). Role of GABA transporter 3 in GABAergic synaptic transmission at striatal output neurons. *Synapse* **63,** 921-9.

KOBAYASHI, M., HAMADA, T., KOGO, M., YANAGAWA, Y., OBATA, K. & KANG, Y. (2008). Developmental profile of GABAA-mediated synaptic transmission in pyramidal cells of the somatosensory cortex. *Eur J Neurosci* **28,** 849-61.

KOCH, U. & MAGNUSSON, A. K. (2009). Unconventional GABA release: mechanisms and function. *Curr Opin Neurobiol* **19,** 305-10.

KOFUJI, P. & NEWMAN, E. A. (2004). Potassium buffering in the central nervous system. *Neuroscience* **129,** 1045-56.

KOIZUMI, S., FUJISHITA, K., TSUDA, M., SHIGEMOTO-MOGAMI, Y. & INOUE, K. (2003). Dynamic inhibition of excitatory synaptic transmission by astrocyte-derived ATP in hippocampal cultures. *Proc Natl Acad Sci U S A* **100,** 11023-8.

KOLE, M. H. & STUART, G. J. (2008). Is action potential threshold lowest in the axon? *Nat Neurosci* **11,** 1253-5.

KONNERTH, A., HEINEMANN, U. & YAARI, Y. (1986). Nonsynaptic epileptogenesis in the mammalian hippocampus in vitro. I. Development of seizurelike activity in low extracellular calcium. *J Neurophysiol* **56,** 409-23.

KOYRAKH, L., LUJAN, R., COLON, J., KARSCHIN, C., KURACHI, Y., KARSCHIN, A. & WICKMAN, K. (2005). Molecular and cellular diversity of neuronal G-protein-gated potassium channels. *J Neurosci* **25,** 11468-78.

KOZLOV, A. S., ANGULO, M. C., AUDINAT, E. & CHARPAK, S. (2006). Target cell-specific modulation of neuronal activity by astrocytes. *Proc Natl Acad Sci U S A* **103,** 10058-63.

KULIK, A., HAENTZSCH, A., LUCKERMANN, M., REICHELT, W. & BALLANYI, K. (1999). Neuron-glia signaling via alpha(1) adrenoceptor-mediated Ca(2+) release in Bergmann glial cells in situ. *J Neurosci* **19,** 8401-8.

KUMARIA, A., TOLIAS, C. M. & BURNSTOCK, G. (2008). ATP signalling in epilepsy. *Purinergic Signal* **4,** 339-46.

LALO, U., PANKRATOV, Y., KIRCHHOFF, F., NORTH, R. A. & VERKHRATSKY, A. (2006). NMDA receptors mediate neuron-to-glia signaling in mouse cortical astrocytes. *J Neurosci* **26,** 2673-83.

LALO, U., PANKRATOV, Y., WICHERT, S. P., ROSSNER, M. J., NORTH, R. A., KIRCHHOFF, F. & VERKHRATSKY, A. (2008). P2X1 and P2X5 subunits form the functional P2X receptor in mouse cortical astrocytes. *J Neurosci* **28,** 5473-80.

LAND, P. W. & SIMONS, D. J. (1985). Cytochrome oxidase staining in the rat SmI barrel cortex. *J Comp Neurol* **238,** 225-35.

LATOUR, I., GEE, C. E., ROBITAILLE, R. & LACAILLE, J. C. (2001). Differential mechanisms of Ca2+ responses in glial cells evoked by exogenous and endogenous glutamate in rat hippocampus. *Hippocampus* **11,** 132-45.

LEE, L. J. & ERZURUMLU, R. S. (2005). Altered parcellation of neocortical somatosensory maps in N-methyl-D-aspartate receptor-deficient mice. *J Comp Neurol* **485,** 57-63.

LEE, S., YOON, B. E., BERGLUND, K., OH, S. J., PARK, H., SHIN, H. S., AUGUSTINE, G. J. & LEE, C. J. (2010). Channel-mediated tonic GABA release from glia. *Science* **330,** 790-6.

LEFORT, S., TOMM, C., FLOYD SARRIA, J. C. & PETERSEN, C. C. (2009). The excitatory neuronal network of the C2 barrel column in mouse primary somatosensory cortex. *Neuron* **61,** 301-16.

LIU, Q. S., XU, Q., KANG, J. & NEDERGAARD, M. (2004). Astrocyte activation of presynaptic metabotropic glutamate receptors modulates hippocampal inhibitory synaptic transmission. *Neuron Glia Biol* **1,** 307-316.

LIU, Q. Y., SCHAFFNER, A. E., CHANG, Y. H., MARIC, D. & BARKER, J. L. (2000). Persistent activation of GABA(A) receptor/Cl(-) channels by astrocyte-derived GABA in cultured embryonic rat hippocampal neurons. *J Neurophysiol* **84,** 1392-403.

LUBKE, J., EGGER, V., SAKMANN, B. & FELDMEYER, D. (2000). Columnar organization of dendrites and axons of single and synaptically coupled excitatory spiny neurons in layer 4 of the rat barrel cortex. *J Neurosci* **20,** 5300-11.

LUBKE, J. & FELDMEYER, D. (2007). Excitatory signal flow and connectivity in a cortical column: focus on barrel cortex. *Brain Struct Funct* **212,** 3-17.

LUBKE, J., ROTH, A., FELDMEYER, D. & SAKMANN, B. (2003). Morphometric analysis of the columnar innervation domain of neurons connecting layer 4 and layer 2/3 of juvenile rat barrel cortex. *Cereb Cortex* **13,** 1051-63.

LUQUE, J. M. & RICHARDS, J. G. (1995). Expression of NMDA 2B receptor subunit mRNA in Bergmann glia. *Glia* **13,** 228-32.

MAGLIONE, M., TRESS, O., HAAS, B., KARRAM, K., TROTTER, J., WILLECKE, K. & KETTENMANN, H. (2010). Oligodendrocytes in mouse corpus callosum are coupled via gap junction channels formed by connexin47 and connexin32. *Glia* **58,** 1104-17.

MARESCAUX, C., VERGNES, M., LIU, Z., DEPAULIS, A. & BERNASCONI, R. (1992). GABAB receptor involvement in the control of genetic absence seizures in rats. *Epilepsy Res Suppl* **9,** 131-8; discussion 138-9.

MARKRAM, H., TOLEDO-RODRIGUEZ, M., WANG, Y., GUPTA, A., SILBERBERG, G. & WU, C. (2004). Interneurons of the neocortical inhibitory system. *Nat Rev Neurosci* **5,** 793-807.

MARTIN, E. D., FERNANDEZ, M., PEREA, G., PASCUAL, O., HAYDON, P. G., ARAQUE, A. & CENA, V. (2007). Adenosine released by astrocytes contributes to hypoxia-induced modulation of synaptic transmission. *Glia* **55,** 36-45.

MATTHIAS, K., KIRCHHOFF, F., SEIFERT, G., HUTTMANN, K., MATYASH, M., KETTENMANN, H. & STEINHAUSER, C. (2003). Segregated expression of AMPA-type glutamate receptors and glutamate transporters defines distinct astrocyte populations in the mouse hippocampus. *J Neurosci* **23,** 1750-8.

MATYASH, V., FILIPPOV, V., MOHRHAGEN, K. & KETTENMANN, H. (2001). Nitric oxide signals parallel fiber activity to Bergmann glial cells in the mouse cerebellar slice. *Mol Cell Neurosci* **18,** 664-70.

MATYASH, V. & KETTENMANN, H. (2010). Heterogeneity in astrocyte morphology and physiology. *Brain Res Rev* **63,** 2-10.

MISGELD, U., BIJAK, M. & JAROLIMEK, W. (1995). A physiological role for GABAB receptors and the effects of baclofen in the mammalian central nervous system. *Prog Neurobiol* **46,** 423-62.

MOTHET, J. P., POLLEGIONI, L., OUANOUNOU, G., MARTINEAU, M., FOSSIER, P. & BAUX, G. (2005). Glutamate receptor activation triggers a calcium-dependent and SNARE protein-dependent release of the gliotransmitter D-serine. *Proc Natl Acad Sci U S A* **102,** 5606-11.

MOUNTCASTLE, V. B. (1997). The columnar organization of the neocortex. *Brain* **120 (Pt 4),** 701-22.

MUTANI, R. (1986). Neurophysiological mechanisms underlying epileptogenesis. *Funct Neurol* **1,** 385-9.

NAVARRETE, M. & ARAQUE, A. (2008). Endocannabinoids mediate neuron-astrocyte communication. *Neuron* **57,** 883-93.

NEDERGAARD, M., RANSOM, B. & GOLDMAN, S. A. (2003). New roles for astrocytes: redefining the functional architecture of the brain. *Trends Neurosci* **26,** 523-30.

NEDERGAARD, M., RODRIGUEZ, J. J. & VERKHRATSKY, A. (2010). Glial calcium and diseases of the nervous system. *Cell Calcium* **47,** 140-9.

NEWMAN, E. A. (2001). Calcium signaling in retinal glial cells and its effect on neuronal activity. *Prog Brain Res* **132,** 241-54.

NEWMAN, E. A. (2004). Glial modulation of synaptic transmission in the retina. *Glia* **47,** 268-74.

NIMMERJAHN, A., KIRCHHOFF, F., KERR, J. N. & HELMCHEN, F. (2004). Sulforhodamine 101 as a specific marker of astroglia in the neocortex in vivo. *Nat Methods* **1,** 31-7.

NOLTE, C., MATYASH, M., PIVNEVA, T., SCHIPKE, C. G., OHLEMEYER, C., HANISCH, U. K., KIRCHHOFF, F. & KETTENMANN, H. (2001). GFAP promoter-controlled EGFP-expressing transgenic mice: a tool to visualize astrocytes and astrogliosis in living brain tissue. *Glia* **33,** 72-86.

ORKAND, R. K., NICHOLLS, J. G. & KUFFLER, S. W. (1966). Effect of nerve impulses on the membrane potential of glial cells in the central nervous system of amphibia. *J Neurophysiol* **29,** 788-806.

PADGETT, C. L. & SLESINGER, P. A. (2010). GABAB receptor coupling to G-proteins and ion channels. *Adv Pharmacol* **58,** 123-47.

PARPURA, V., BASARSKY, T. A., LIU, F., JEFTINIJA, K., JEFTINIJA, S. & HAYDON, P. G. (1994). Glutamate-mediated astrocyte-neuron signalling. *Nature* **369,** 744-7.

PASCUAL, O., CASPER, K. B., KUBERA, C., ZHANG, J., REVILLA-SANCHEZ, R., SUL, J. Y., TAKANO, H., MOSS, S. J., MCCARTHY, K. & HAYDON, P. G. (2005). Astrocytic purinergic signaling coordinates synaptic networks. *Science* **310,** 113-6.

PASTI, L., VOLTERRA, A., POZZAN, T. & CARMIGNOTO, G. (1997). Intracellular calcium oscillations in astrocytes: a highly plastic, bidirectional form of communication between neurons and astrocytes in situ. *J Neurosci* **17,** 7817-30.

PEINADO, A., YUSTE, R. & KATZ, L. C. (1993). Extensive dye coupling between rat neocortical neurons during the period of circuit formation. *Neuron* **10,** 103-14.

PEREA, G. & ARAQUE, A. (2005). Properties of synaptically evoked astrocyte calcium signal reveal synaptic information processing by astrocytes. *J Neurosci* **25,** 2192-203.

PEREA, G. & ARAQUE, A. (2007). Astrocytes potentiate transmitter release at single hippocampal synapses. *Science* **317,** 1083-6.

PEREA, G., NAVARRETE, M. & ARAQUE, A. (2009). Tripartite synapses: astrocytes process and control synaptic information. *Trends Neurosci* **32,** 421-31.

PETERS, A. & HARRIMAN, K. M. (1988). Enigmatic bipolar cell of rat visual cortex. *J Comp Neurol* **267,** 409-32.

PETERS, O., SCHIPKE, C. G., HASHIMOTO, Y. & KETTENMANN, H. (2003). Different mechanisms promote astrocyte Ca2+ waves and spreading depression in the mouse neocortex. *J Neurosci* **23,** 9888-96.

PETERS, O., SCHIPKE, C. G., PHILIPPS, A., HAAS, B., PANNASCH, U., WANG, L. P., BENEDETTI, B., KINGSTON, A. E. & KETTENMANN, H. (2009). Astrocyte function is modified by Alzheimer's disease-like pathology in aged mice. *J Alzheimers Dis* **18,** 177-89.

PETRAVICZ, J., FIACCO, T. A. & MCCARTHY, K. D. (2008). Loss of IP3 receptor-dependent Ca2+ increases in hippocampal astrocytes does not affect baseline CA1 pyramidal neuron synaptic activity. *J Neurosci* **28,** 4967-73.

PORTER, J. T. & MCCARTHY, K. D. (1996). Hippocampal astrocytes in situ respond to glutamate released from synaptic terminals. *J Neurosci* **16,** 5073-81.

PORTER, J. T. & MCCARTHY, K. D. (1997). Astrocytic neurotransmitter receptors in situ and in vivo. *Prog Neurobiol* **51,** 439-55.

POWELL, K. L., NG, C., O'BRIEN, T. J., XU, S. H., WILLIAMS, D. A., FOOTE, S. J. & REID, C. A. (2008). Decreases in HCN mRNA expression in the hippocampus after kindling and status epilepticus in adult rats. *Epilepsia* **49,** 1686-95.

PRIEST, C. A., THOMPSON, A. J. & KELLER, A. (2001). Gap junction proteins in inhibitory neurons of the adult barrel neocortex. *Somatosens Mot Res* **18,** 245-52.

RADNIKOW, G., FELDMEYER, D. & LUBKE, J. (2002). Axonal projection, input and output synapses, and synaptic physiology of Cajal-Retzius cells in the developing rat neocortex. *J Neurosci* **22,** 6908-19.

RIVERA, C., VOIPIO, J. & KAILA, K. (2005). Two developmental switches in GABAergic signalling: the K+-Cl- cotransporter KCC2 and carbonic anhydrase CAVII. *J Physiol* **562,** 27-36.

ROERIG, B. & FELLER, M. B. (2000). Neurotransmitters and gap junctions in developing neural circuits. *Brain Res Brain Res Rev* **32,** 86-114.

RORIG, B. & SUTOR, B. (1996). Regulation of gap junction coupling in the developing neocortex. *Mol Neurobiol* **12,** 225-49.

SCHIPKE, C. G., HAAS, B. & KETTENMANN, H. (2008). Astrocytes discriminate and selectively respond to the activity of a subpopulation of neurons within the barrel cortex. *Cereb Cortex* **18,** 2450-9.

SCHOUSBOE, A. (2003). Role of astrocytes in the maintenance and modulation of glutamatergic and GABAergic neurotransmission. *Neurochem Res* **28,** 347-52.

SCHUMMERS, J., YU, H. & SUR, M. (2008). Tuned responses of astrocytes and their influence on hemodynamic signals in the visual cortex. *Science* **320,** 1638-43.

SEIFERT, G., CARMIGNOTO, G. & STEINHAUSER, C. (2010). Astrocyte dysfunction in epilepsy. *Brain Res Rev* **63,** 212-21.

SEIFERT, G., SCHILLING, K. & STEINHAUSER, C. (2006). Astrocyte dysfunction in neurological disorders: a molecular perspective. *Nat Rev Neurosci* **7,** 194-206.

SEIFERT, G. & STEINHAUSER, C. (1995). Glial cells in the mouse hippocampus express AMPA receptors with an intermediate Ca2+ permeability. *Eur J Neurosci* **7,** 1872-81.

SEIFERT, G. & STEINHAUSER, C. (2001). Ionotropic glutamate receptors in astrocytes. *Prog Brain Res* **132,** 287-99.

SERRANO, A., HADDJERI, N., LACAILLE, J. C. & ROBITAILLE, R. (2006). GABAergic network activation of glial cells underlies hippocampal heterosynaptic depression. *J Neurosci* **26,** 5370-82.

SHIGETOMI, E., KRACUN, S., SOFRONIEW, M. V. & KHAKH, B. S. (2010). A genetically targeted optical sensor to monitor calcium signals in astrocyte processes. *Nat Neurosci* **13,** 759-66.

SHLEPER, M., KARTVELISHVILY, E. & WOLOSKER, H. (2005). D-serine is the dominant endogenous coagonist for NMDA receptor neurotoxicity in organotypic hippocampal slices. *J Neurosci* **25,** 9413-7.

SIDORYK-WEGRZYNOWICZ, M., WEGRZYNOWICZ, M., LEE, E., BOWMAN, A. B. & ASCHNER, M. (2011). Role of astrocytes in brain function and disease. *Toxicol Pathol* **39,** 115-23.

SIMONS, D. J. & WOOLSEY, T. A. (1984). Morphology of Golgi-Cox-impregnated barrel neurons in rat SmI cortex. *J Comp Neurol* **230,** 119-32.

SOMOGYI, P. & COWEY, A. (1981). Combined Golgi and electron microscopic study on the synapses formed by double bouquet cells in the visual cortex of the cat and monkey. *J Comp Neurol* **195,** 547-66.

SOMOGYI, P., TAMAS, G., LUJAN, R. & BUHL, E. H. (1998). Salient features of synaptic organisation in the cerebral cortex. *Brain Res Brain Res Rev* **26,** 113-35.

SONTHEIMER, H. (1994). Voltage-dependent ion channels in glial cells. *Glia* **11,** 156-72.

STELLWAGEN, D. & MALENKA, R. C. (2006). Synaptic scaling mediated by glial TNF-alpha. *Nature* **440,** 1054-9.

SUN, Q. Q., ZHANG, Z., JIAO, Y., ZHANG, C., SZABO, G. & ERDELYI, F. (2009). Differential metabotropic glutamate receptor expression and modulation in two neocortical inhibitory networks. *J Neurophysiol* **101,** 2679-92.

SUTOR, B. & LUHMANN, H. J. (1998). Involvement of GABA(B) receptors in convulsant-induced epileptiform activity in rat neocortex in vitro. *Eur J Neurosci* **10,** 3417-27.

SUTULA, T. P., CAVAZOS, J. E. & WOODARD, A. R. (1994). Long-term structural and functional alterations induced in the hippocampus by kindling: implications for memory dysfunction and the development of epilepsy. *Hippocampus* **4,** 254-8.

SWADLOW, H. A. (2002). Thalamocortical control of feed-forward inhibition in awake somatosensory 'barrel' cortex. *Philos Trans R Soc Lond B Biol Sci* **357,** 1717-27.

SZATKOWSKI, M., BARBOUR, B. & ATTWELL, D. (1990). Non-vesicular release of glutamate from glial cells by reversed electrogenic glutamate uptake. *Nature* **348,** 443-6.

TAKATA, N. & HIRASE, H. (2008). Cortical layer 1 and layer 2/3 astrocytes exhibit distinct calcium dynamics in vivo. *PLoS One* **3,** e2525.

TEICHGRABER, L. A., LEHMANN, T. N., MEENCKE, H. J., WEISS, T., NITSCH, R. & DEISZ, R. A. (2009). Impaired function of GABA(B) receptors in tissues from pharmacoresistant epilepsy patients. *Epilepsia* **50,** 1697-716.

THEIS, M., JAUCH, R., ZHUO, L., SPEIDEL, D., WALLRAFF, A., DORING, B., FRISCH, C., SOHL, G., TEUBNER, B., EUWENS, C., HUSTON, J., STEINHAUSER, C., MESSING, A., HEINEMANN, U. & WILLECKE, K. (2003). Accelerated hippocampal spreading depression and enhanced locomotory activity in mice with astrocyte-directed inactivation of connexin43. *J Neurosci* **23,** 766-76.

UVAROV, P., LUDWIG, A., MARKKANEN, M., PRUUNSILD, P., KAILA, K., DELPIRE, E., TIMMUSK, T., RIVERA, C. & AIRAKSINEN, M. S. (2007). A novel N-terminal isoform of the neuron-specific K-Cl cotransporter KCC2. *J Biol Chem* **282,** 30570-6.

VERDERIO, C., BRUZZONE, S., ZOCCHI, E., FEDELE, E., SCHENK, U., DE FLORA, A. & MATTEOLI, M. (2001). Evidence of a role for cyclic ADP-ribose in calcium signalling and neurotransmitter release in cultured astrocytes. *J Neurochem* **78,** 646-57.

VERGNES, M., BOEHRER, A., SIMLER, S., BERNASCONI, R. & MARESCAUX, C. (1997). Opposite effects of GABAB receptor antagonists on absences and convulsive seizures. *Eur J Pharmacol* **332,** 245-55.

VERKHRATSKY, A. (2006). Calcium ions and integration in neural circuits. *Acta Physiol (Oxf)* **187,** 357-69.

VERKHRATSKY, A. & KETTENMANN, H. (1996). Calcium signalling in glial cells. *Trends Neurosci* **19,** 346-52.

VERKHRATSKY, A., ORKAND, R. K. & KETTENMANN, H. (1998). Glial calcium: homeostasis and signaling function. *Physiol Rev* **78,** 99-141.

VERKHRATSKY, A. & STEINHAUSER, C. (2000). Ion channels in glial cells. *Brain Res Brain Res Rev* **32,** 380-412.

VOLTERRA, A. & STEINHAUSER, C. (2004). Glial modulation of synaptic transmission in the hippocampus. *Glia* **47,** 249-57.

WALLRAFF, A., KOHLING, R., HEINEMANN, U., THEIS, M., WILLECKE, K. & STEINHAUSER, C. (2006). The impact of astrocytic gap junctional coupling on potassium buffering in the hippocampus. *J Neurosci* **26,** 5438-47.

WANG, X., LOU, N., XU, Q., TIAN, G. F., PENG, W. G., HAN, X., KANG, J., TAKANO, T. & NEDERGAARD, M. (2006). Astrocytic Ca2+ signaling evoked by sensory stimulation in vivo. *Nat Neurosci* **9,** 816-23.

WANG, Y., GUPTA, A., TOLEDO-RODRIGUEZ, M., WU, C. Z. & MARKRAM, H. (2002). Anatomical, physiological, molecular and circuit properties of nest basket cells in the developing somatosensory cortex. *Cereb Cortex* **12,** 395-410.

WANG, Y., TOLEDO-RODRIGUEZ, M., GUPTA, A., WU, C., SILBERBERG, G., LUO, J. & MARKRAM, H. (2004). Anatomical, physiological and molecular properties of Martinotti cells in the somatosensory cortex of the juvenile rat. *J Physiol* **561,** 65-90.

WARR, O., TAKAHASHI, M. & ATTWELL, D. (1999). Modulation of extracellular glutamate concentration in rat brain slices by cystine-glutamate exchange. *J Physiol* **514 (Pt 3),** 783-93.

WELKER, C. & WOOLSEY, T. A. (1974). Structure of layer IV in the somatosensory neocortex of the rat: description and comparison with the mouse. *J Comp Neurol* **158,** 437-53.

WHITE, E. L. & ROCK, M. P. (1980). Three-dimensional aspects and synaptic relationships of a Golgi-impregnated spiny stellate cell reconstructed from serial thin sections. *J Neurocytol* **9,** 615-36.

WOOLSEY, T. A. & VAN DER LOOS, H. (1970). The structural organization of layer IV in the somatosensory region (SI) of mouse cerebral cortex. The description of a cortical field composed of discrete cytoarchitectonic units. *Brain Res* **17,** 205-42.

YE, Z. C., WYETH, M. S., BALTAN-TEKKOK, S. & RANSOM, B. R. (2003). Functional hemichannels in astrocytes: a novel mechanism of glutamate release. *J Neurosci* **23,** 3588-96.

ZEILHOFER, H. U., STUDLER, B., ARABADZISZ, D., SCHWEIZER, C., AHMADI, S., LAYH, B., BOSL, M. R. & FRITSCHY, J. M. (2005). Glycinergic neurons expressing enhanced green fluorescent protein in bacterial artificial chromosome transgenic mice. *J Comp Neurol* **482,** 123-41.

ZHANG, J. M., WANG, H. K., YE, C. Q., GE, W., CHEN, Y., JIANG, Z. L., WU, C. P., POO, M. M. & DUAN, S. (2003). ATP released by astrocytes mediates glutamatergic activity-dependent heterosynaptic suppression. *Neuron* **40,** 971-82.

ZHU, L., LOVINGER, D. & DELPIRE, E. (2005). Cortical neurons lacking KCC2 expression show impaired regulation of intracellular chloride. *J Neurophysiol* **93,** 1557-68.

ZHU, Y., STORNETTA, R. L. & ZHU, J. J. (2004). Chandelier cells control excessive cortical excitation: characteristics of whisker-evoked synaptic responses of layer 2/3 nonpyramidal and pyramidal neurons. *J Neurosci* **24,** 5101-8.

INDEX

Page:

27. RESULTS

27. Morphological and physiological properties of selected neurons

29. Neuronal coupling

30. Evoked response in and outside the stimulated column

33. Ca^{2+} chelation in astrocytes

35. BAPTA dialysis of astrocytes impaired their Ca^{2+} response locally but a large population of astrocytes was activated in a distal region

38. Astrocytic Ca^{2+} chelation leads to an enhanced neuronal evoked response

41. Activation of $GABA_A$ and $GABA_B$ receptors inhibits neuronal evoked response

43. Astrocytic Ca^{2+} chelation, GABA receptor blockage or dialysis with high $[Cl^-]$ reverse a stimulus-induced hyperpolarization into depolarization

45. Astrocytic Ca^{2+} chelation increases the frequency of APs after stimulation (high $[Cl^-]_i$ in neuron)

46. Neuronal reversal potential shifts from -50 to 0mV upon GABA receptors blockage

48. Neurons dialyzed with high $[Cl^-]$ show spontaneous depolarizing events after astrocytes were dialyzed with BAPTA

50. $GABA_B$-mediated neuronal inhibition

52. Ionotropic glutamate receptor blockers have an only marginal effect on the neuronal evoked response

63. DISCUSSION

CURRICULUM VITAE

Mein Lebenslauf wird aus datenschutzrechtlichen Gründen in der elektronischen Version meiner Arbeit nicht veröffentlicht

Erklärung

„Ich, Bruno Benedetti, erkläre, dass ich die vorgelegte Dissertation mit dem Thema: „Astrocytes control GABAergic inhibition of neurons in the mouse barrel cortex“ selbst verfasst und keine anderen als die angegebenen Quellen und Hilfsmittel benutzt, ohne die (unzulässige) Hilfe Dritter verfasst und auch in Teilen keine Kopien anderer Arbeiten dargestellt habe.“

Datum Unterschrift